Biophysical *Journal*
Computational Tool

Biophysical Society

Metapredict: a fast, accurate, and easy-to-use predictor of consensus disorder and structure

Ryan J. Emenecker,[1,2,3] Daniel Griffith,[1,2] and Alex S. Holehouse[1,2,*]
[1]Department of Biochemistry and Molecular Biophysics, Washington University School of Medicine, St. Louis, Missouri; [2]Center for Science and Engineering Living Systems (CSELS) and [3]Center for Engineering Mechanobiology, Washington University, St. Louis, Missouri

ABSTRACT Intrinsically disordered proteins and protein regions make up a substantial fraction of many proteomes in which they play a wide variety of essential roles. A critical first step in understanding the role of disordered protein regions in biological function is to identify those disordered regions correctly. Computational methods for disorder prediction have emerged as a core set of tools to guide experiments, interpret results, and develop hypotheses. Given the multiple different predictors available, consensus scores have emerged as a popular approach to mitigate biases or limitations of any single method. Consensus scores integrate the outcome of multiple independent disorder predictors and provide a per-residue value that reflects the number of tools that predict a residue to be disordered. Although consensus scores help mitigate the inherent problems of using any single disorder predictor, they are computationally expensive to generate. They also necessitate the installation of multiple different software tools, which can be prohibitively difficult. To address this challenge, we developed a deep-learning-based predictor of consensus disorder scores. Our predictor, metapredict, utilizes a bidirectional recurrent neural network trained on the consensus disorder scores from 12 proteomes. By benchmarking metapredict using two orthogonal approaches, we found that metapredict is among the most accurate disorder predictors currently available. Metapredict is also remarkably fast, enabling proteome-scale disorder prediction in minutes. Importantly, metapredict is a fully open source and is distributed as a Python package, a collection of command-line tools, and a web server, maximizing the potential practical utility of the predictor. We believe metapredict offers a convenient, accessible, accurate, and high-performance predictor for single-proteins and proteomes alike.

SIGNIFICANCE Intrinsically disordered regions are found across all kingdoms of life, in which they play a variety of essential roles. Being able to accurately and quickly identify disordered regions in proteins using just the amino acid sequence is critical for the appropriate design and interpretation of experiments. Despite this, performing large-scale disorder prediction on thousands of sequences is challenging using extant disorder predictors due to various difficulties, including general installation and computational requirements. We have developed an accurate, high-performance, and easy-to-use predictor of protein disorder and structure. Our predictor, metapredict, was designed for both proteome-scale analysis and individual sequence predictions alike. Metapredict is implemented as a collection of local tools and an online web server and is appropriate for both seasoned computational biologists and novices alike.

INTRODUCTION

Although it is often convenient to consider proteins as nanoscopic molecular machines, such a description betrays many of their functionally critical features (1–3). As an extreme example, intrinsically disordered proteins and protein regions (collectively referred to as IDRs) do not adopt a fixed three-dimensional conformation (4–8). Instead, IDRs exist in an ensemble of different conformations that are in exchange with one another (9–11). Despite the absence of a well-defined structured state, IDRs are integral to many important biological processes (12,13). As a result, there is a growing appreciation for the importance of disordered regions across the three kingdoms of life (6,12,14,15).

A key first step in exploring the role of disorder in biological function is the identification of disordered regions. Although IDRs can be formally identified by various biophysical methods (including nuclear magnetic resonance spectroscopy, circular dichroism, or single-molecule spectroscopy), these techniques can be challenging and are

Submitted May 27, 2021, and accepted for publication August 30, 2021.
*Correspondence: alex.holehouse@wustl.edu
Editor: Jianhan Chen.
https://doi.org/10.1016/j.bpj.2021.08.039

generally low throughput (16–18). As implied by the name, the "intrinsically" disordered nature of IDRs reflects the fact that these protein regions are unable to fold into a well-defined tertiary structure in isolation. This is in contrast to folded regions, which under appropriate solution conditions adopt macroscopically similar three-dimensional structures (19–21). The complexities of metastability in protein folding notwithstanding, this definition implies that this intrinsic ability to fold (or not fold) is encoded by the primary amino acid sequence (22–24). As such, it should be possible to delineate between folded and disordered regions based solely on amino acid sequence.

The prediction of protein disorder from amino acid sequence has received considerable attention for over 20 years, driven by pioneering early work by Dunker et al. (6–8,25,26). Since those original bioinformatics tools, a wide range of disorder predictors have emerged (27–30). Accurate disorder predictors offer an approach to guide experimental design, interpret data, and build testable hypotheses. As such, the application of disorder predictors to assess predicted protein structure has become a relatively standard type of analysis, although the specific predictor used varies depending on availability, simplicity, and scope of the question.

There are currently many disorder predictors that apply different approaches to predict protein disorder. These range from statistical approaches based on structural data from the protein data bank, to biophysical methods that consider local "foldability," to machine learning-based algorithms trained on experimentally determined disordered sequences (31–38). However, using any individual predictor can be problematic; each predictor has specific biases and weaknesses in its capacity to accurately predict protein disorder, which can introduce systematic biases into large-scale disorder assessment (39). As such, an alternative strategy in which many different predictors are combined to offer a consensus disorder score has emerged as a popular alternative to relying on any specific predictor (40–44). Consensus scores report the fraction of independent disorder predictors that would predict a given residue as disordered: for example, a score of 0.5 reports that 50% of predictors predict that residue to be disordered.

Although using consensus scores mitigates the limitations of any single predictor, calculating consensus scores is computationally expensive and necessitates the installation of multiple distinct software packages. To alleviate this challenge, consensus disorder scores can be precomputed and held in online-accessible databases (42,45–47). Although precomputed scores are an invaluable resource to the scientific community their application is limited to a small subset of possible sequences. Furthermore, obtaining, managing, and analyzing large datasets of precomputed consensus predictions can be a daunting task, especially if only a subset of sequences are of interest.

To address these challenges, we have developed a fast, accurate, and simple-to-use deep learning-based disorder predictor trained on precomputed consensus scores from a range of organisms. Our resulting predictor, metapredict, is platform agnostic, simple to install, and usable as a Python module, a stand-alone command-line tool, or as a stand-alone web server. Metapredict accurately reproduces consensus disorder scores and is sufficiently fast such that for most bioinformatics pipelines, precomputation of disorder is no longer necessary, and disorder can be computed in real-time as analysis is performed. In addition to consensus disorder prediction, metapredict also provides structure confidence scores based on AlphaFold2-derived predictions of folding propensity, a related but complementary mode of sequence annotation. Metapredict can be installed in seconds, is incredibly lightweight, and has no specific hardware requirements. Taken together, metapredict is a high-performance and easy-to-use disorder predictor appropriate for computational novices to seasoned bioinformaticians alike.

MATERIALS AND METHODS

Training metapredict using PARROT

To create metapredict, we used PARROT (Protein Analysis using RecuRrent neural networks On Training data), a general-purpose deep learning toolkit developed for mapping between sequence annotations and sequence (48). PARROT was used to train a bidirectional recurrent neural network with long short-term memory (LSTM) on the disorder consensus scores from the MobiDB database for each residue for all of the proteins in 12 proteomes (see Supporting materials and methods for details) (Fig. 1) (48–50). The eight disorder predictors used to generate the consensus scores in the MobiDB database were IUPred short (34), IUPred long (34), ESpiritz (DisProt, NMR, and x ray) (31), DisEMBL 465 (28), DisEMBL hot loops (28), and GlobPlot (51). In total, metapredict was trained using almost 300,000 individual protein sequences. For AlphaFold2-based predictions, the per-residue predicted local difference test (pLDDT) score from 21 different proteomes were used as input (see Supporting materials and methods for details) (52,53). The pLDDT score reflects the confidence AlphaFold2 has in the local structure prediction.

Recurrent neural networks are well-suited for protein sequence machine learning tasks due to their ability to directly parse sequences of variable length without modification (54). Bidirectionality is a common modification of recurrent neutral networks and is particularly relevant in the context of sequence-based prediction because it ensures that the entire local sequence (both N- and C-terminal) is accounted for when making the disorder prediction of a particular residue. Finally, LSTM networks are another common modification of recurrent neutral networks that have seen widespread adoption in machine learning tasks because of their improved ability to retain long-range information over the course of training (50). Consequently, bidirectional LSTMs have emerged as a powerful class of deep learning model for sequence-based predictions (48,55–57).

To determine the optimal threshold to delineate disordered and ordered regions, we systematically varied the cutoff score used to classify IDRs (Figs. S4–S8). This analysis revealed that a broad range of cutoffs (between 0.2 and 0.4) gave approximately equivalent performance, such that a cutoff of 0.3 offered a good balance between true positives and false negatives. As such, IDRs identified by metapredict with the default setting can be treated as relatively high-confidence, at the expense of missing some cryptic disordered regions.

Usage and features

Metapredict is offered in three distinct formats (Fig. S9). As a downloadable package, it can be used either via a set of command-line tools or as

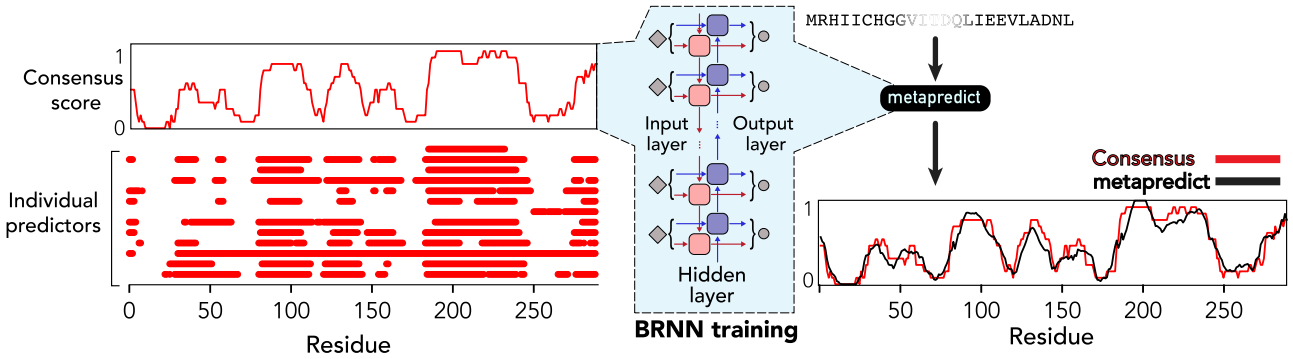

FIGURE 1 Overview of metapredict. Consensus scores are taken from 420,660 proteins distributed across 12 proteomes. Metapredict was developed by training a bidirectional recurrent neural network (BRNN) on this data, leading to a set of network weights that allow the prediction of any possible consensus sequence score.

a Python module. Command-line predictions include functionality to directly predict disorder from a UniProt accession, save disorder scores as a text file, and predict disorder for multiple sequences within an FASTA file. The Python module includes the ability to predict per-residue consensus disorder scores or delineate continuous IDRs. Complete documentation is available at http://metapredict.readthedocs.io/. In addition, we offer a web server appropriate for individual protein sequences, which is available at http://metapredict.net.

Performance

On all hardware tested (which included a laptop from 2012), metapredict obtained prediction rates of ~7000–12,000 residues per second (see Supporting materials and methods for further details). A single 300-residue protein takes ~25 ms, and the human proteome (20,396 sequences) takes ~21 min. Importantly and unlike some other predictors, the computational cost scales linearly with sequence length (Fig. S6) (58).

RESULTS

Evaluating metapredict accuracy in comparison to existing predictors

Given the large number of protein disorder predictors available, multiple groups have investigated different approaches to measure their accuracy (27,59–61). Here, we used metrics from two recent studies, allowing us to compare directly with many previously evaluated predictors.

We first evaluated metapredict using the protocol developed for the Critical Assessment of Protein Intrinsic Disorder experiment (CAID; 652 sequences). CAID is a biennial event in which a large set of protein disorder predictors are assessed using a standardized dataset and standardized metrics (27). CAID uses a curated dataset of 646 proteins from DisProt, a database of experimentally validated disordered regions (62). As such, evaluation using CAID's standards offers a convenient route to benchmark metapredict against the state of the art.

In keeping with the assessments developed by CAID, we evaluated metapredict in its capacity to predict disorder across two distinct datasets (DisProt, DisProt-Protein Database (PDB)) as well as its ability to identify fully disordered proteins (27). Although DisProt contains only true positive disordered regions, DisProt-PDB contains true positive and true negative regions, making it more appropriate for robust validation of discriminatory predictors (27). To maintain consistency with CAID, we used the F1-score (defined as the maximum harmonic mean between precision and recall across all threshold values; Eq. S3) to compare metapredict against other predictors (27). The F1-score of metapredict in the analysis of the DisProt dataset ranked 12th highest out of the 38 predictors originally assessed (Fig. 2 *A*).

DisProt contains protein subregions that have been experimentally validated as disordered. However, as noted in the original study, it is possible, if not likely, that there are other subregions from those same proteins which, although not yet annotated as such, are in fact disordered (27). The DisProt-PDB dataset addresses this limitation and includes only protein regions that are unambiguously annotated as either disordered or ordered based on extant experimental data (27). In examining the performance of metapredict in predicting disorder on the DisProt-PDB dataset, we found that metapredict ranked 11th among all of the disorder predictors assessed (Fig. 2 *B*).

The last analysis that we carried out from the CAID experiment was the capacity of metapredict to identify fully disordered proteins. In this context, the CAID experiment considers something to be a fully disordered protein if the disorder predictor predicts 95% or more residues to be disordered (27). Metapredict ranked third out of the disorder predictors examined in its capacity to identify fully disordered proteins (Fig. 2 *C*).

In addition to assessing metapredict via the CAID dataset, we also evaluated metapredict using the chemical shift *z*-score for assessing order/disorder, an alternative metric that provides a per-residue continuous value that experimentally quantifies disorder (see Supporting materials and methods for more details) (61). Similar to the CAID-based assessment, metapredict ranked on average eighth out of 23 predictors (Fig. S1).

Although our assessment thus far is consistent with prior metrics, we worried that it lacked clear interpretability with

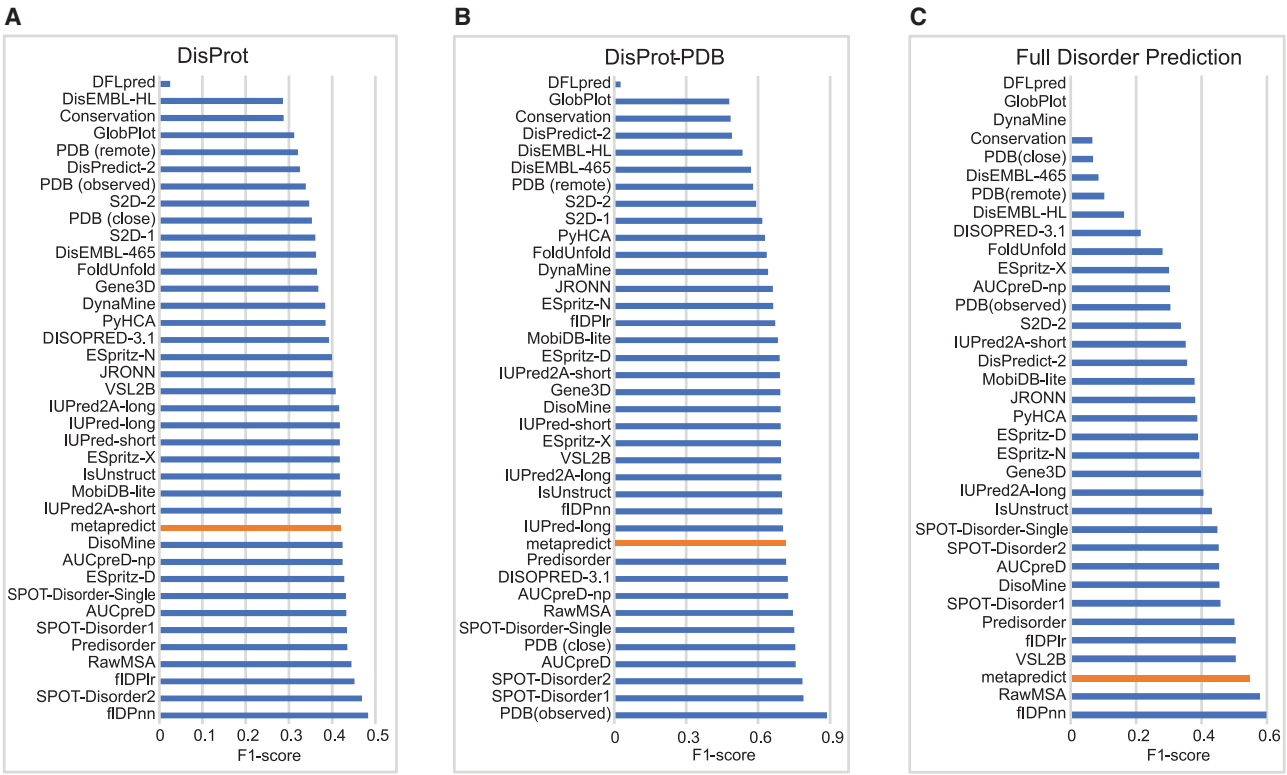

FIGURE 2 Evaluation of metapredict using CAID experiments. (*A*) F1-score for various predictors in examining their accuracy in predicting protein disorder from the DisProt dataset. (*B*) F1-scores for various predictors in examining their accuracy in predicting protein disorder from the DisProt-PDB dataset. (*C*) F1-scores for various predictors in predicting fully disordered proteins in the DisProt dataset. Values for all predictors in (*A*)–(*C*) with the exception of those for metapredict (*orange bar*) were obtained from (27).

respect to what these measures of accuracy mean for real protein sequences. To address this, we re-evaluated the CAID-derived predictions to compute an accuracy score that reflects the number of residues correctly predicted as folded or disordered per 100, using a Disprot-PDB-like dataset with any ambiguous residues excluded. Fig. 3 *A* shows the resulting assessment and reveals that although the general order obtained from other methods is preserved (as expected), the difference between the best predictor and metapredict is on average two residues per 100.

Evaluating metapredict execution time in comparison to existing predictors

Next, we considered how long metapredict takes to predict disorder compared with other predictors. AUCpreD was one of the top-performing disorder predictors, and compared to several other top predictors was relatively easy to install. We evaluated the computational cost per-residue using the command-line version of metapredict. The time for AUCpreD-based disorder prediction scaled linearly with sequence length with ∼0.3 s per residue (e.g., a 2151-residue protein takes ∼14 min) (Fig. S2). In contrast, no metapredict sequence took more than 0.9 s. In fact, for single-sequence predictions, the main determinant of metapredict time was the time to load the trained network file (∼0.6 s) that, when predicting an FASTA file with multiple sequences, is a fixed and negligible computational cost. When this was accounted for, metapredict takes ∼0.02 s for a 300-residue protein (Fig. S8).

The CAID competition quantified execution times for 32 predictors using standardized hardware, providing a rigorous and complete assessment of relative performance. By scaling our hardware based on the CAID execution time scores for AUCPreD, we were able to compare the accuracy and qualitative execution time of metapredict against all 32 predictors for the full CAID assessment (Fig. 3 *B*). Although metapredict was ∼2 residues per 100 less accurate than the top-performing predictor, it took ∼40 s to predict disorder for the full CAID dataset, compared with approximately one month. We tentatively suggest this difference in execution time compensates for difference in accuracy (Fig. S10).

Prediction of AlphaFold2 pLDDT prediction

In addition to direct disorder prediction and in response to the release of AlphaFold2-derived structure predictions for multiple proteomes, we developed a predictor for the per-residue confidence scores derived from the AlphaFold2

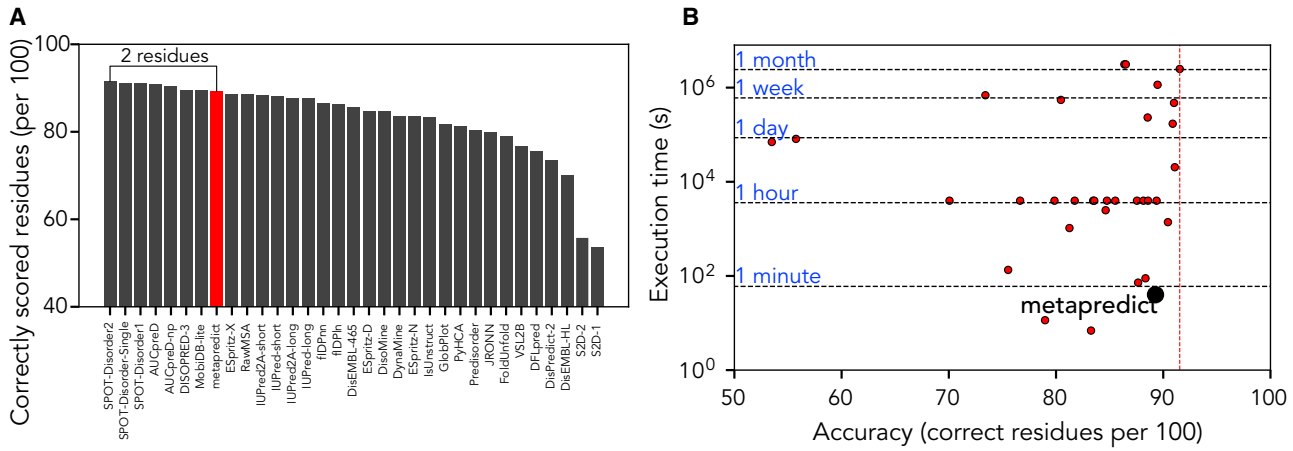

FIGURE 3 Accuracy and performance of metapredict. (*A*) Rank order of predictors in terms of number of correct residues per 100, assessed using true positive and true negative only (Disprot-PDB dataset). (*B*) Relative execution time for all predictors as evaluated in CAID over 652 independent sequences. Metapredict emerges as the third fastest predictor with a relative average loss in accuracy of two residues per 100 compared with the state-of-the-art (see also Fig. S11.)

dataset (see Supporting materials and methods for more details) (52,53). Formally, these scores reflect a pLDDT, such that metapredict offers a predicted prediction (i.e., a predicted pLDDT score) (Fig. 4 *A*). Given the acquisition of structure can be considered the inverse of disorder, we expect (and observe) an anticorrelation between predicted structure confidence and disorder (Fig. 4 *B*; Fig. S3). We provide this feature as a complementary tool to aid in the interpretation of disorder scores, a feature that we anticipate will be useful when assessing ambiguous regions.

DISCUSSION

IDRs play vital roles in various biological processes (12,13). An essential first step in the investigation of IDR function reflects the ability to identify IDRs within a protein sequence. Consensus disorder scores represent an attractive means by which to obtain high confidence disorder predictions that do not suffer from inaccuracies due to the limitations of any single-disorder predictor. However, calculating disorder probabilities from many different predictors to generate a consensus score is cumbersome, technically challenging, and computationally expensive. To address this, we developed metapredict, a simple to use protein disorder predictor that accurately reproduces consensus disorder scores. Although other consensus metapredictors do exist, web-based access to these can be on the order of minutes-to-hours per sequence and, where available, local access has operating-system dependencies making them poorly suited to cross-platform proteome-scale analysis (41,64,65). As such, we believe metapredict fills a niche that is currently unoccupied.

Metapredict makes use of a general approach in machine learning known as knowledge distillation. In knowledge distillation, a computationally cheap model is trained on data generated by one (or more) computationally expensive models, with a limited loss of accuracy (66,67). This approach entirely detaches metapredict from either the computational cost or the computational complexity of other models, minimizing execution time, installation challenges, and limitations with respect to software or operating system dependencies.

In comparison with the other disorder predictors, metapredict tended to err on the side of false-negative predictions (where metapredict predicted something to be ordered when it was in fact disordered). As such, metapredict appears to possess a slight bias toward underestimating disorder, such that IDRs identified by metapredict can be considered reasonably high confidence. Although metapredict is not the most accurate disorder predictor, we tentatively suggest the average error of two residues in 100 is relatively small. To aid in delineation between regions that may be ambiguous, the AlphaFold2 predicted structure confidence offers an orthogonal approach that provides additional discriminatory power.

Features of metapredict

To further aid in the identification of bona fide contiguous disordered regions, metapredict contains a stand-alone function for extracting contiguous IDRs based on a threshold value applied to a smoothed disorder score and several additional parameters (Figs. S4–S7). For this approach, we again found a threshold between 0.3 and 0.4 was optimal, and this method generally outperformed our prior more simple analyses. However, because other predictors did not use this approach for domain classification we also chose not to use it in examining the accuracy of metapredict. Nonetheless, this suggests that metapredict can achieve even marginally higher accuracy in identifying IDRs and automates this procedure for the users, allowing boundaries between IDRs and folded domains to be automatically identified, greatly facilitating IDR-ome style analyses of datasets.

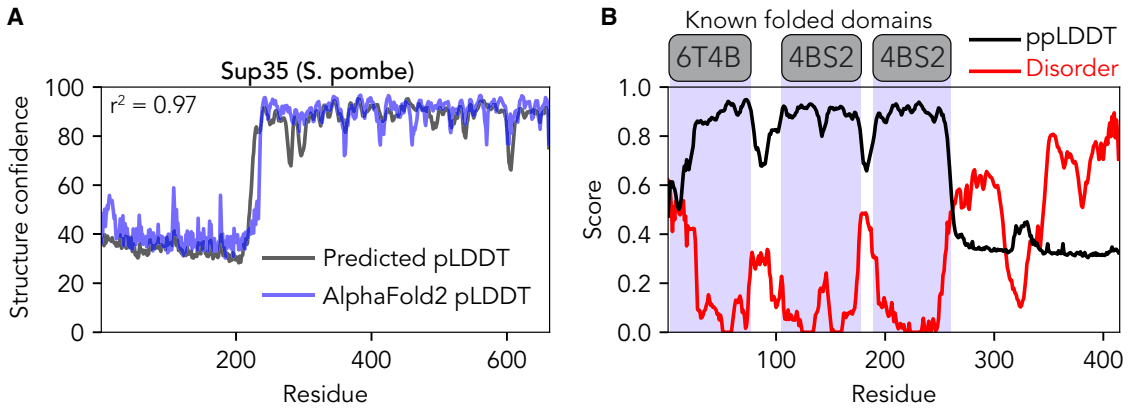

FIGURE 4 Metapredict also offers predicted structure confidence based on AlphaFold2. (*A*) Comparison of predicted pLDDT (*blue*) versus actual pLDDT for the translational termination factor Sup35 from *Schizosaccharomyces pombe*. This sequence was not used in the training data, and is provided as a simple illustrative example of the agreement between the metapredict-derived prediction and actual AlphaFold2 pLDDT values (*B*). Comparison of disorder (*red*), predicted pLDDT (ppLDDT; divided by 100 to place it on the same scale), and known folded domains (*gray* and *blue*) with associated Protein Data Bank IDs shown for the human RNA-binding protein TDP-43. The C-terminal disordered region is an experimentally verified IDR (63). Disorder and ppLDDT scores are anticorrelated and correctly identify domain boundaries.

In addition to disorder prediction and in response to the recent release of AlphaFold2, metapredict offers an additional predictor of structure trained on AlphaFold2 data. The implications and application of AlphaFold2-derived predicted structure is an ongoing topic of investigation for many groups (68–71). Although the absence of predicted structure cannot "necessarily" be taken to mean a region is disordered, there is a strong correlation and good reason to believe that for proteins in isolation, regions lacking high-confidence predicted structure may be disordered (Fig. S3) (52,53). As a final thought, predicting structure confidence using metapredict takes milliseconds, making this a potential screening tool for identifying high-confidence sequences of interest which could be investigated using the full AlphaFold2 methodology.

As a final note, an important feature in the distribution of software is the ease of installation. Metapredict can be installed through a single terminal command ("pip install metapredict"), all dependencies are automatically included, and the metapredict package is just 3.8 MBs. This is in contrast to many other state-of-the-art predictors, which require large sets of additional tools (each of which must be separately installed) and hundreds of gigabytes of database files, and provide execution times on the order of minutes to hours per sequence. We believe metapredict offers an accurate, convenient, and computationally efficient approach to de novo disorder prediction.

Code and data availability

The code for metapredict can be found at: https://github.com/idptools/metapredict. Documentation is available at https://metapredict.readthedocs.io/. Fully processed sequences used for assessment (including sequences and scores) and code used for this manuscript are provided at https://github.com/holehouse-lab/supportingdata/. Metapredict can be installed directly from the Python Packaging Index using pip (i.e., "pip install metapredict").

SUPPORTING MATERIAL

Supporting material can be found online at https://doi.org/10.1016/j.bpj.2021.08.039.

AUTHOR CONTRIBUTIONS

R.J.E. designed research, developed code, performed analysis, made figures, and wrote the initial manuscript. D.G. developed code, performed analysis, made figures, and wrote the manuscript. A.S.H. designed research, developed code, made figures, and wrote the manuscript.

ACKNOWLEDGMENTS

We thank Ishan Taneja and Jeff Lotthammer for helpful comments on the manuscript, and FNZ for extensive discussions. We thank Steven Boeynaems for the "motivation" to develop our web server. We thank DeepMind and EBI for providing all the AlphaFold2 data in such an accessible, robust, and timely manner. We also thank the entire Tosatto group, the ELIXIR Intrinsically Disordered Proteins Community, and HUPO-PSI Intrinsically Disordered Proteins Community (notably Silvio Tosatto, Zsuzsanna Dosztanyi, Damiano Piovesan, Wim Vranken, and Norman Davey) for all the European-funded bioinformatics work that largely fuels the international internsically disordered proteins informatics space.

Funding for this project was provided by the Longer Life Foundation (an RGA/Washington University Collaboration) to A.S.H., National Science Foundation Graduate Research Fellowship DGE-2139839 to D.G., and the William H. Danforth Plant Science Fellowship to R.J.E.

REFERENCES

1. Sormanni, P., D. Piovesan, …, M. Vendruscolo. 2017. Simultaneous quantification of protein order and disorder. *Nat. Chem. Biol.* 13:339–342.

2. Bottaro, S., and K. Lindorff-Larsen. 2018. Biophysical experiments and biomolecular simulations: a perfect match? *Science.* 361:355–360.
3. Henzler-Wildman, K., and D. Kern. 2007. Dynamic personalities of proteins. *Nature.* 450:964–972.
4. van der Lee, R., M. Buljan, …, M. M. Babu. 2014. Classification of intrinsically disordered regions and proteins. *Chem. Rev.* 114:6589–6631.
5. Wright, P. E., and H. J. Dyson. 1999. Intrinsically unstructured proteins: re-assessing the protein structure-function paradigm. *J. Mol. Biol.* 293:321–331.
6. Dunker, A. K., Z. Obradovic, …, C. J. Brown. 2000. Intrinsic protein disorder in complete genomes. *Genome Inform. Ser. Workshop Genome Inform.* 11:161–171.
7. Uversky, V. N. 2002. Natively unfolded proteins: a point where biology waits for physics. *Protein Sci.* 11:739–756.
8. Tompa, P. 2002. Intrinsically unstructured proteins. *Trends Biochem. Sci.* 27:527–533.
9. Mittag, T., and J. D. Forman-Kay. 2007. Atomic-level characterization of disordered protein ensembles. *Curr. Opin. Struct. Biol.* 17:3–14.
10. Forman-Kay, J. D., and T. Mittag. 2013. From sequence and forces to structure, function, and evolution of intrinsically disordered proteins. *Structure.* 21:1492–1499.
11. Mao, A. H., N. Lyle, and R. V. Pappu. 2013. Describing sequence-ensemble relationships for intrinsically disordered proteins. *Biochem. J.* 449:307–318.
12. Wright, P. E., and H. J. Dyson. 2015. Intrinsically disordered proteins in cellular signalling and regulation. *Nat. Rev. Mol. Cell Biol.* 16:18–29.
13. Oldfield, C. J., and A. K. Dunker. 2014. Intrinsically disordered proteins and intrinsically disordered protein regions. *Annu. Rev. Biochem.* 83:553–584.
14. Tompa, P., and M. Fuxreiter. 2008. Fuzzy complexes: polymorphism and structural disorder in protein-protein interactions. *Trends Biochem. Sci.* 33:2–8.
15. Tompa, P., and A. Fersht. 2009. Structure and Function of Intrinsically Disordered Proteins. CRC Press, New York.
16. Gibbs, E. B., E. C. Cook, and S. A. Showalter. 2017. Application of NMR to studies of intrinsically disordered proteins. *Arch. Biochem. Biophys.* 628:57–70.
17. Chemes, L. B., L. G. Alonso, …, G. de Prat-Gay. 2012. Circular dichroism techniques for the analysis of intrinsically disordered proteins and domains. *Methods Mol. Biol.* 895:387–404.
18. Schuler, B., A. Soranno, …, D. Nettels. 2016. Single-molecule FRET spectroscopy and the polymer physics of unfolded and intrinsically disordered proteins. *Annu. Rev. Biophys.* 45:207–231.
19. Karplus, M., and D. L. Weaver. 1976. Protein-folding dynamics. *Nature.* 260:404–406.
20. Anfinsen, C. B. 1973. Principles that govern the folding of protein chains. *Science.* 181:223–230.
21. Dill, K. A., and H. S. Chan. 1997. From Levinthal to pathways to funnels. *Nat. Struct. Biol.* 4:10–19.
22. Honeycutt, J. D., and D. Thirumalai. 1990. Metastability of the folded states of globular proteins. *Proc. Natl. Acad. Sci. USA.* 87:3526–3529.
23. Thirumalai, D., and G. Reddy. 2011. Protein thermodynamics: are native proteins metastable? *Nat. Chem.* 3:910–911.
24. Hu, X., L. Hong, …, J. C. Smith. 2016. The dynamics of single protein molecules is non-equilibrium and self-similar over thirteen decades in time. *Nat. Phys.* 12:171–174.
25. Romero, P., Z. Obradovic, …, A. K. Dunker. 1997. Identifying disordered regions in proteins from amino acid sequence. *In* Proceedings of International Conference on Neural Networks (ICNN'97), pp. 90–95.
26. Romero, O., Obradovic, and K. Dunker. 1997. Sequence data analysis for long disordered regions prediction in the calcineurin family. Genome Inform. Ser. *Workshop Genome Inform.* 8:110–124.
27. Necci, M., D. Piovesan, S. C. E. Tosatto; CAID Predictors; DisProt Curators. 2021. Critical assessment of protein intrinsic disorder prediction. *Nat. Methods.* 18:472–481.
28. Linding, R., L. J. Jensen, …, R. B. Russell. 2003. Protein disorder prediction: implications for structural proteomics. *Structure.* 11:1453–1459.
29. Ferron, F., S. Longhi, …, D. Karlin. 2006. A practical overview of protein disorder prediction methods. *Proteins.* 65:1–14.
30. Deng, X., J. Eickholt, and J. Cheng. 2012. A comprehensive overview of computational protein disorder prediction methods. *Mol. Biosyst.* 8:114–121.
31. Walsh, I., A. J. M. Martin, …, S. C. E. Tosatto. 2012. ESpritz: accurate and fast prediction of protein disorder. *Bioinformatics.* 28:503–509.
32. Mészáros, B., G. Erdős, and Z. Dosztányi. 2018. IUPred2A: context-dependent prediction of protein disorder as a function of redox state and protein binding. *Nucleic Acids Res.* 46:W329–W337.
33. Dosztányi, Z., V. Csizmók, …, I. Simon. 2005. The pairwise energy content estimated from amino acid composition discriminates between folded and intrinsically unstructured proteins. *J. Mol. Biol.* 347:827–839.
34. Dosztányi, Z., V. Csizmok, …, I. Simon. 2005. IUPred: web server for the prediction of intrinsically unstructured regions of proteins based on estimated energy content. *Bioinformatics.* 21:3433–3434.
35. Dass, R., F. A. A. Mulder, and J. T. Nielsen. 2020. ODiNPred: comprehensive prediction of protein order and disorder. *Sci. Rep.* 10:14780.
36. Hanson, J., K. K. Paliwal, …, Y. Zhou. 2019. SPOT-Disorder2: improved protein intrinsic disorder prediction by ensembled deep learning. *Genomics Proteomics Bioinformatics.* 17:645–656.
37. Ishida, T., and K. Kinoshita. 2007. PrDOS: prediction of disordered protein regions from amino acid sequence. *Nucleic Acids Res.* 35:W460–W464.
38. Mizianty, M. J., Z. Peng, and L. Kurgan. 2013. MFDp2: accurate predictor of disorder in proteins by fusion of disorder probabilities, content and profiles. *Intrinsically Disord. Proteins.* 1:e24428.
39. Katuwawala, A., C. J. Oldfield, and L. Kurgan. 2020. Accuracy of protein-level disorder predictions. *Brief. Bioinform.* 21:1509–1522.
40. Necci, M., D. Piovesan, …, S. C. E. Tosatto. 2017. MobiDB-lite: fast and highly specific consensus prediction of intrinsic disorder in proteins. *Bioinformatics.* 33:1402–1404.
41. Kozlowski, L. P., and J. M. Bujnicki. 2012. MetaDisorder: a meta-server for the prediction of intrinsic disorder in proteins. *BMC Bioinformatics.* 13:111.
42. Piovesan, D., M. Necci, …, S. C. E. Tosatto. 2021. MobiDB: intrinsically disordered proteins in 2021. *Nucleic Acids Res.* 49:D361–D367.
43. Necci, M., D. Piovesan, …, S. C. E. Tosatto. 2020. MobiDB-lite 3.0: fast consensus annotation of intrinsic disorder flavors in proteins. *Bioinformatics.* 36:5533–5534.
44. Peng, Z., and L. Kurgan. 2012. On the complementarity of the consensus-based disorder prediction. *Pac. Symp. Biocomput* 176–187.
45. Di Domenico, T., I. Walsh, and S. C. E. Tosatto. 2013. Analysis and consensus of currently available intrinsic protein disorder annotation sources in the MobiDB database. *BMC Bioinformatics.* 14 (*Suppl 7*):S3.
46. Oates, M. E., P. Romero, …, J. Gough. 2013. D^2P^2: database of disordered protein predictions. *Nucleic Acids Res.* 41:D508–D516.
47. Potenza, E., T. Di Domenico, …, S. C. E. Tosatto. 2015. MobiDB 2.0: an improved database of intrinsically disordered and mobile proteins. *Nucleic Acids Res.* 43:D315–D320.
48. Griffith, D., and A. S. Holehouse. 2021. PARROT: a flexible recurrent neural network framework for analysis of large protein datasets. *bioRxiv* https://doi.org/10.1101/2021.05.21.445045.
49. Piovesan, D., F. Tabaro, …, S. C. E. Tosatto. 2018. MobiDB 3.0: more annotations for intrinsic disorder, conformational diversity and interactions in proteins. *Nucleic Acids Res.* 46:D471–D476.

50. Hochreiter, S., and J. Schmidhuber. 1997. Long short-term memory. *Neural Comput.* 9:1735–1780.

51. Linding, R., R. B. Russell, …, T. J. Gibson. 2003. GlobPlot: exploring protein sequences for globularity and disorder. *Nucleic Acids Res.* 31:3701–3708.

52. Tunyasuvunakool, K., J. Adler, …, D. Hassabis. 2021. Highly accurate protein structure prediction for the human proteome. *Nature.* 596:590–596.

53. Jumper, J., R. Evans, …, D. Hassabis. 2021. Highly accurate protein structure prediction with AlphaFold. *Nature.* 596:583–589.

54. Min, S., B. Lee, and S. Yoon. 2017. Deep learning in bioinformatics. *Brief. Bioinform.* 18:851–869.

55. Li, S., J. Chen, and B. Liu. 2017. Protein remote homology detection based on bidirectional long short-term memory. *BMC Bioinformatics.* 18:443.

56. Almagro Armenteros, J. J., C. K. Sønderby, …, O. Winther. 2017. DeepLoc: prediction of protein subcellular localization using deep learning. *Bioinformatics.* 33:3387–3395.

57. Hanson, J., Y. Yang, …, Y. Zhou. 2017. Improving protein disorder prediction by deep bidirectional long short-term memory recurrent neural networks. *Bioinformatics.* 33:685–692.

58. Goodfellow, I., Y. Bengio, …, Y. Bengio. 2016. Deep Learning. MIT Press, Cambridge, MA.

59. Monastyrskyy, B., K. Fidelis, …, A. Kryshtafovych. 2011. Evaluation of disorder predictions in CASP9. *Proteins.* 79 (*Suppl 10*):107–118.

60. Monastyrskyy, B., A. Kryshtafovych, …, K. Fidelis. 2014. Assessment of protein disorder region predictions in CASP10. *Proteins.* 82 (*Suppl 2*):127–137.

61. Nielsen, J. T., and F. A. A. Mulder. 2019. Quality and bias of protein disorder predictors. *Sci. Rep.* 9:5137.

62. Hatos, A., B. Hajdu-Soltész, …, D. Piovesan. 2020. DisProt: intrinsic protein disorder annotation in 2020. *Nucleic Acids Res.* 48:D269–D276.

63. Conicella, A. E., G. H. Zerze, …, N. L. Fawzi. 2016. ALS mutations disrupt phase separation mediated by α-helical structure in the TDP-43 low-complexity C-terminal domain. *Structure.* 24:1537–1549.

64. Schlessinger, A., M. Punta, …, B. Rost. 2009. Improved disorder prediction by combination of orthogonal approaches. *PLoS One.* 4:e4433.

65. Xue, B., R. L. Dunbrack, …, V. N. Uversky. 2010. PONDR-FIT: a meta-predictor of intrinsically disordered amino acids. *Biochim. Biophys. Acta.* 1804:996–1010.

66. Kim, Y., and A. M. Rush. 2016. Sequence-level knowledge distillation. *arXiv*, arXiv:1606.07947 http://arxiv.org/abs/1606.07947.

67. Hinton, G., O. Vinyals, and J. Dean. 2015. Distilling the knowledge in a neural network. *arXiv*, arXiv:1503.02531 http://arxiv.org/abs/1503.02531.

68. Jehl, P., J. Manguy, …, N. E. Davey. 2016. ProViz-a web-based visualization tool to investigate the functional and evolutionary features of protein sequences. *Nucleic Acids Res.* 44:W11–W15.

69. Tsaban, T., J. Varga, …, O. Schueler-Furman. 2021. Harnessing protein folding neural networks for peptide-protein docking. *bioRxiv* https://doi.org/10.1101/2021.08.01.454656.

70. McCoy, A. J., M. D. Sammito, and R. J. Read. 2021. Possible implications of AlphaFold2 for crystallographic phasing by molecular replacement. *bioRxiv* https://doi.org/10.1101/2021.05.18.444614.

71. Ko, J., and J. Lee. 2021. Can AlphaFold2 predict protein-peptide complex structures accurately? *bioRxiv* https://doi.org/10.1101/2021.07.27.453972.

Biophysical Journal, Volume *120*

Supplemental information

Metapredict: a fast, accurate, and easy-to-use predictor of consensus disorder and structure

Ryan J. Emenecker, Daniel Griffith, and Alex S. Holehouse

Supplemental Information:
metapredict: a fast, accurate, and easy-to-use predictor of consensus disorder and structure

Ryan J. Emenecker[1, 2, 3], Daniel Griffith[1, 2], Alex S. Holehouse[1, 2*]

1. Department of Biochemistry and Molecular Biophysics, Washington University School of Medicine, St. Louis, MO, 63100, USA
2. Center for Science and Engineering Living Systems (CSELS), Washington University, St. Louis, MO 63130, USA
3. Center for Engineering Mechanobiology, Washington University, St. Louis, MO 63130, USA

* Correspondence: alex.holehouse@wustl.edu

Supplemental Materials and Methods

Evaluating metapredict using CheZOD scores

In line with previous work, we assessed how the continuous probability values of various predictors correlated with the CheZOD scores using the Pearson's correlation coefficient (Eq. 1) (Nielsen & Mulder, 2019). CheZOD scores increase with order and decrease with disorder. A Pearson's correlation coefficient of −1 would mean that a predictor is perfectly anti-correlated with the Z-scores, and 0 would mean that there is no correlation. As such, the results are displayed as the absolute value of the Pearson Correlation coefficient.

Based on the CheZOD, metapredict ranked 8th among the 23 predictors previously examined (**Supplemental Fig. 1A**). We also calculated the area under a receiver operating characteristic curve (AUC). The receiver operating characteristic curve uses true positive values and false positive values to assess the accuracy of the various predictors, such that a perfect predictor would have an AUC of 1. Based on this assessment metapredict was ranked 11th out of the 23 predictors evaluated (**Supplemental Fig. 1B**).

We next examined the accuracy of metapredict in predicting binary classification of either order or disorder. Previously, a CheZOD score of less than 8 was considered disordered (Nielsen & Mulder, 2019). When converting a metapredict score to binary classification, we considered any residue with a score of 0.3 or higher as disordered. For this analysis the Matthews Correlation Coefficient (MCC) was also calculated for each predictor (Eq. 2). The MCC uses a combination of false positives, false negatives, true positives, and true negatives in order to examine the accuracy of a classifier. We found that metapredict had the 8th highest MCC out of the predictors evaluated (**Supplemental Table 1**).

Metapredict implementation and usage

metapredict is written in Python 3.7+ and uses PyTorch, with the initial network trained using PARROT (Griffith & Holehouse, 2021; Paszke et al., 2019).

We designed metapredict to be as flexible and user-friendly as possible. For example, metapredict can be used as a Python library (**Supplemental Fig. 8A**), a stand-alone command-line tool (**Supplemental Fig. 8B**) or a web server (http://metapredict.net) (**Supplemental Fig. 8C**). Moreover, metapredict contains functionality to generate graphs or disorder scores from the command-line by directly inputting a single protein sequence, a UniProt accession number, or a FASTA file containing many sequences. Finally, in comparison to other predictors, which can take seconds, minutes or even hours per sequence, metapredict's computational performance makes it sufficiently fast that on-the-fly disorder prediction can be faster than reading pre-computed values from disk. It is this combination of accuracy, computational efficiency, ease of use, and flexibility that makes metapredict a convenient tool for any kind of disorder prediction, from single sequences to proteome-wide analyses.

To illustrate the ability of metapredict to predict consensus scores, **Supplemental Fig. 9** shows the computed consensus scores and the analogous prediction for four proteins with IDRs. Across our datasets, we found that metapredict generally performed better than over two-thirds of the currently available disorder predictors examined, likely with a slight bias for false negatives when the default disorder threshold is applied.

For a list of features see the documentation at https://metapredict.readthedocs.io/.

Evaluating metapredict disorder scores

Evaluations and datasets for the CheZOD score analysis (116 sequences) can be found in (Nielsen & Mulder, 2019). Evaluations and datasets for the Critical Assessment of protein Intrinsic Disorder prediction (CAID) analysis (652 sequences) can be found in (Necci et al., 2021). For convenience, all sequences and scores used are also provided at https://github.com/holehouse-lab/supportingdata/. All values are also found in **Supplemental tables 1-8**. Details on results including additional statistical analyses and the raw performance scores for each predictor that was used for comparisons to metapredict can be found in the supporting materials and methods.

Statistical analysis for evaluating the accuracies of disorder predictors

Statistical analysis and predictor evaluation was carried out following the protocols described previously and reproduced here for completeness (Necci et al., 2021; Nielsen & Mulder, 2019).

Predictor evaluation is performed via the Pearson's Correlation coefficient (R_p), the Matthew's Correlation Coefficient (MCC), and the F1-score.

The Pearson's Correlation Coefficient (R_p) is calculated as,

$$R_p = \frac{\sum(x_i - x_a)(y_i - y_a)}{\sqrt{\sum(x_i - x_a)^2 \sum(y_i - y_a)^2}} \qquad \text{(Eq. 1)}$$

where x_i is the value of the current predicted disorder value for a residue in a sequence, x_a is the mean predicted disorder value for the residues in a sequence, y_i is the actual disorder value (specifically the CheZOD score) of the current residue, and y_a is the mean actual disorder value.

The Matthew's Correlation Coefficient (MCC) is calculated as,

$$MCC = \frac{(TP \times TN) - (FP \times FN)}{\sqrt{(TP + FP) \times (TN + FP) \times (TP + FN) \times (TN + FN)}} \quad \text{(Eq. 2)}$$

Where true positives (TP) are the number of times a disorder predictor predicts a disordered residue to be disordered, true negatives (TN) are the number of times a predictor does not predict something to be disordered when it is not disordered, false positives (FP) are the number of times a predictor predicts a residue to be disordered when it is in fact not disordered, and false negatives (FN) are the number of times a predictor predicts a residue to not be disordered when it is in fact disordered.

Finally, the F1-score is calculated as

$$\text{F1-score} = \frac{TP}{TP + (0.5 \times (FP + FN))} \quad \text{(Eq. 3)}$$

Where TP, FP, and FN are defined above.

Metapredict training of disorder predictor

The metapredict disorder prediction was trained using PARROT with slight modifications to the default settings (Griffith & Holehouse, 2021). We set the number of training epochs, which defines the number of times the complete dataset is assessed and used to update the network parameters, to 100. Increasing the number of epochs further gave a negligible improvement in performance. The PARROT data type was set to 'residues' and the number of classes was set to '1' (for regression). The learning rate (--learning-rate), which is a parameter that alters the rate that the model updates weights after each round of back-propagation, was set to 0.001. The number of layers (--num-layers), which is the number of layers in the network between the input layer and the output layer, was set to 1. The hidden vector size (--hidden-size), which is the size of hidden vectors within the BRNN, was set to 5. The batch size (--batch), which is the number of sequences processed at the same time, was set to 32. For training, validation, and testing, 70% of the data was used for training, 15% of the data was used for validation, and 15% of the data was used for testing.

The proteomes for which consensus disorder scores were available at the time of training were: *Danio rerio* (UP000000437, 43,841 proteins), *Gallus gallus* (UP000000539, 25,238), *Mus*

musculus (UP000000589, 44,470 proteins), *Drosophila melanogaster* (UP000000803, 21,114 proteins), *Dictyostelium discoideum* (UP000002195, 12,733 proteins), *Canis lupus familiaris* (UP000002254, 45,089 proteins), *Saccharomyces cerevisiae* (UP000002311, 6,049 proteins), *Rattus norvegicus* (UP000002494, 29,090 proteins), *Homo sapiens* (UP000005640, 66,835), *Arabidopsis thaliana* (UP000006548, 39,342 proteins), *Sus scrofa* (UP000008227, 49,792 proteins), and *Bos taurus* (UP000009136, 37,367 proteins). These numbers reflect protein sequences composed of the 20 standard amino acids only. Cross-referencing the training dataset (70% of the total sequences) taken from these proteomes against the assessment databases used (CheZOD and CAID) identified 28/116 from CheZOD and 451/652 from CAID databases in a total training set of ~295,000 sequences. These proteomes and the associated consensus disorder scores were obtained from MobiDB, but were originally curated by UniProt (Acids Research & 2021, 2021; Piovesan et al., 2021; UniProt Consortium, 2019).

Metapredict performance

Metapredict has no specific hardware requirements and performs well across all set ups tested. Hardware tested included an Unbuntu-running Dell desktop (Ubuntu 18.04 with Intel(R) Core(TM) i9-9900 CPU @ 3.10GHz CPU, 32 GBs DDR4 RAM, with a Toshiba 512 GB SSD (KBG40ZNS512G), a 2020 Apple Mac Mini (16 GB unified memory, Apple M1 processor), a 2019 16-inch MacBook Pro (64 GB 2667 MHz DDR4 RAM, 2.3 GHz Intel Core i9 processor, Intel UHD Graphics 630 integrated graphics), and a 2012 MacBook Pro (2.9 GHz Intel Core i7 processor, 8 GB 1600 MHz DDR3 RAM, Intel HD Graphics 4000 1536 MB integrated graphics). Importantly, as evident by our testing on a 2012 MacBook Pro (which scored at 7,238 residues per second), metapredict does not require a high-end modern computer to be fast. Even on the most basic virtual machine available, (Ubuntu 18.04 with single virtual Intel CPU (2.4 GHz), 1 GB DIMM memory, 20 GB SSD), metapredict performs at ~6000 residues per second.

To compare AUCPreD vs. metapredict (**Supplemental Fig. S1**) predictions were performed on a desktop machine running Ubuntu 18.04 with an Intel(R) Core(TM) i9-9900 CPU @ 3.10GHz CPU, 32 GBs DDR4 RAM, with a Toshiba 512 GB SSD (KBG40ZNS512G). To ensure a fair comparison, each sequence was isolated and placed in its own FASTA file, and the predictor ran on each file independently. In reality, if one had multiple sequences, placing them into a single FASTA file would be a more efficient approach to minimize the amount of time reading from the filesystem. While the effective contribution of file read time is negligible for AUCPreD, in all cases for metapredict it is the dominant determinant of execution time.

To compare metapredict execution time against other predictors based on times reported in the CAID experiment, we used per-sequence execution times for AUCPreD on our local hardware and on the CAID hardware to calibrate and approximate conversion factor. A more detailed explanation of this process is described in https://github.com/holehouse-lab/supportingdata/tree/master/2021/emenecker_metapredict_2021/performance/metapredict_on_caid_disprot

AlphaFold2 pLDDT predictor data

We obtained pLDDT scores for every AlphaFold2 model from http://ftp.ebi.ac.uk/pub/databases/alphafold/ and extracted the pLDDT score from these models for twenty one proteomes (UP000002485_284812_SCHPO, UP000000805_243232_METJA, UP000001450_36329_PLAF7, UP000005640_9606_HUMAN, UP000001584_83332_MYCTU, UP000001940_6239_CAEEL, UP000000625_83333_ECOLI, UP000002296_353153_TRYCC, UP000000803_7227_DROME, UP000007305_4577_MAIZE, UP000002195_44689_DICDI, UP000002311_559292_YEAST, UP000002494_10116_RAT, UP000008153_5671_LEIIN, UP000008816_93061_STAA8, UP000006548_3702_ARATH, UP000008827_3847_SOYBN, UP000000437_7955_DANRE, UP000000589_10090_MOUSE, UP000059680_39947_ORYSJ, UP000000559_237561_CANAL). For each of these proteomes all PDB models were used, with the exception of the human proteome where only the first (F1) models were used. In total 363,264 different sequences were used.

AlphaFold2 pLDDT predictor training

The AlphaFold2 (AF2) pLDDT predictor (alphaPredict) was trained using PARROT (version 1.5.0), the same general-purpose deep learning framework used to create the BRNN behind the metapredict disorder predictions. The parameters used for PARROT training were as follows: residues datatype, 1 class (for regression), a learning-rate of 0.001, 2 hidden layers, 20 hidden vectors, a batch size of 32, and 200 training epochs.

AlphaFold2 pLDDT predictor accuracy

At the time of writing, our AF2 pLDDT confidence score predictor obtained an r^2 value for the actual versus predicted scores in the test set was 0.7148 and the average error per residue was approximately 9.20% (network V4).

AlphaFold2 pLDDT predictor implementation

For improved modularity, the AlphaFold2 predictor is currently implemented as a separate Python package (alphaPredict) which is encoded as a silent dependency to metapredict (https://github.com/ryanemenecker/alphaPredict). alphaPredict can also be downloaded and used independently from metapredict in its own right. alphaPredict is written in Python 3.7+ and uses PyTorch, with the initial network trained using PARROT (Griffith & Holehouse, 2021; Paszke et al., 2019).

AlphaFold2 pLDDT predictor improvements

The prior information regarding the network (network V2) used for the AF2 pLDDT confidence score predictions in metapredict is up to date at the time of this writing. However, additional networks (a V3 and V4) are currently in progress. However, due to the increased number of proteomes used for training these networks and the slightly altered parameters, they currently have weeks of additional training remaining before completion. For the most up to date information on the AF2 pLDDT prediction in metapredict, please see https://github.com/ryanemenecker/alphaPredict.

Supplemental Tables

	Rp	AUC	MCC	TPR	TNR	FPR	FNR	prec	Acc
SPOT-dis	-0.657	0.881	0.59089	0.7067	0.8757	0.1243	0.2933	0.9177	0.7912
MFDp2	-0.631	0.853	0.578	0.8528	0.7275	0.2725	0.1472	0.8599	0.7901
MetaDisorder	-0.617	0.865	0.541	0.8221	0.7287	0.2713	0.1779	0.856	0.7754
AUCpreD	-0.598	0.865	0.54	0.7154	0.8555	0.1445	0.2846	0.9066	0.7854
MetaDisorderMD2	-0.614	0.852	0.54	0.7688	0.7955	0.2045	0.2312	0.8806	0.7821
MetaDisorderMD	-0.616	0.853	0.519	0.7246	0.8227	0.1773	0.2754	0.8891	0.7736
IUPred_long	-0.566	0.834	0.512	0.7477	0.7887	0.2113	0.2523	0.8741	0.7682
AUCpreD_noEvo	-0.512	0.841	0.48658	0.603	0.8664	0.1336	0.397	0.8985	0.7347
metapredict	-0.559	0.832	0.489	0.790	0.718	0.282	0.210	0.860	0.754
DISPROT (VSL2b)	-0.536	0.808	0.466	0.8525	0.5986	0.4014	0.1475	0.8064	0.7256
RONN	-0.5	0.804	0.455	0.7387	0.7368	0.2632	0.2613	0.8463	0.7377
DISOPRED3	-0.551	0.833	0.451	0.5301	0.9207	0.0793	0.4699	0.9292	0.7254
IUPred_short	-0.532	0.822	0.429	0.6284	0.8249	0.1751	0.3716	0.8756	0.7267
ESpritz_DisProt	-0.419	0.748	0.412	0.8208	0.5846	0.4154	0.1792	0.7949	0.7027
PrDOS	-0.541	0.836	0.409	0.5333	0.889	0.111	0.4667	0.9041	0.7111
ESpritz_NMR	-0.478	0.797	0.374	0.4662	0.9087	0.0913	0.5338	0.9092	0.6874
DISpro	-0.437	0.805	0.35712	0.3185	0.9565	0.0435	0.6815	0.9349	0.6375
DISOPRED2	-0.33	0.738	0.3419	0.642	0.6994	0.3006	0.358	0.8073	0.6707
MetaDisorder3D	-0.361	0.727	0.333	0.5841	0.7674	0.2326	0.4159	0.8312	0.6757
DisEMBL_coils	-0.404	0.735	0.32932	0.7252	0.6016	0.3984	0.2748	0.7812	0.6634
ESpritz_Xray	-0.438	0.791	0.286	0.282	0.9597	0.0403	0.718	0.9321	0.6208
DisEMBL_remark465	-0.386	0.737	0.284	0.4219	0.8598	0.1402	0.5781	0.8551	0.6409
DisEMBL_hotloops	-0.286	0.702	0.239	0.432	0.8093	0.1907	0.568	0.8163	0.6206

Supplemental Table 1. CHEZOD scores obtained from (Nielsen & Mulder, 2019).

	Rankings				
Rank	Rp	AUC	MCC	prec	Acc
1	SPOT-dis	SPOT-dis	SPOT-dis	DISpro	SPOT-dis
2	MFDp2	AUCpreD	MFDp2	ESpritz_Xray	MFDp2
3	MetaDisorder	MetaDisorder	MetaDisorder	DISOPRED3	AUCpreD
4	MetaDisorderMD	MFDp2	AUCpreD	SPOT-dis	MetaDisorderMD2
5	MetaDisorderMD2	MetaDisorderMD	MetaDisorderMD2	ESpritz_NMR	MetaDisorder
6	AUCpreD	MetaDisorderMD2	MetaDisorderMD	AUCpreD	MetaDisorderMD
7	IUPred_long	AUCpreD_noEvo	IUPred_long	PrDOS	IUPred_long
8	metapredict	PrDOS	metapredict	AUCpreD_noEvo	metapredict
9	DISOPRED3	IUPred_long	AUCpreD_noEvo	MetaDisorderMD	RONN
10	PrDOS	DISOPRED3	DISPROT (VSL2b)	MetaDisorderMD2	AUCpreD_noEvo
11	DISPROT (VSL2b)	metapredict	RONN	IUPred_short	IUPred_short
12	IUPred_short	IUPred_short	DISOPRED3	IUPred_long	DISPROT (VSL2b)
13	AUCpreD_noEvo	DISPROT (VSL2b)	IUPred_short	MFDp2	DISOPRED3
14	RONN	DISpro	ESpritz_DisProt	metapredict	PrDOS
15	ESpritz_NMR	RONN	PrDOS	MetaDisorder	ESpritz_DisProt
16	ESpritz_Xray	ESpritz_NMR	ESpritz_NMR	DisEMBL_remark465	ESpritz_NMR
17	DISpro	ESpritz_Xray	DISpro	RONN	MetaDisorder3D
18	ESpritz_DisProt	ESpritz_DisProt	DISOPRED2	MetaDisorder3D	DISOPRED2
19	DisEMBL_coils	DISOPRED2	MetaDisorder3D	DisEMBL_hotloops	DisEMBL_coils
20	DisEMBL_remark465	DisEMBL_remark465	DisEMBL_coils	DISOPRED2	DisEMBL_remark465
21	MetaDisorder3D	DisEMBL_coils	ESpritz_Xray	DISPROT (VSL2b)	DISpro
22	DISOPRED2	MetaDisorder3D	DisEMBL_remark465	ESpritz_DisProt	ESpritz_Xray
23	DisEMBL_hotloops	DisEMBL_hotloops	DisEMBL_hotloops	DisEMBL_coils	DisEMBL_hotloops

Supplemental Table 2. CHEZOD-based rankings. This table is provided in a .xlsx format at the manuscript's GitHub repository.

	TN	FP	FN	TP	MCC	F1-s	TNR	TPR	PPV	BAC
flDPnn	585	16	19	26	0.569	0.598	0.973	0.578	0.619	0.776
RawMSA	582	19	19	26	0.546	0.578	0.968	0.578	0.578	0.773
VSL2B	578	23	22	23	0.468	0.505	0.962	0.511	0.5	0.736
flDPlr	566	35	18	27	0.468	0.505	0.942	0.6	0.435	0.771
Predisorder	589	12	26	19	0.479	0.5	0.98	0.422	0.613	0.701
SPOT-Disorder1	572	29	23	22	0.416	0.458	0.952	0.489	0.431	0.72
DisoMine	551	50	17	28	0.421	0.455	0.917	0.622	0.359	0.77
AUCpreD	588	13	28	17	0.431	0.453	0.978	0.378	0.567	0.678
SPOT-Disorder2	574	27	24	21	0.409	0.452	0.955	0.467	0.438	0.711
metapredict	599	8	25	20	0.539	0.548	0.987	0.444	0.714	0.716
SPOT-Disorder-Single	594	7	30	15	0.452	0.448	0.988	0.333	0.682	0.661
IsUnstruct	588	13	29	16	0.411	0.432	0.978	0.356	0.552	0.667
IUPred2A-long	595	6	32	13	0.42	0.406	0.99	0.289	0.684	0.639
Gene3D	505	96	10	35	0.391	0.398	0.84	0.778	0.267	0.809
ESpritz-N	597	4	33	12	0.426	0.393	0.993	0.267	0.75	0.63
ESpritz-D	555	46	23	22	0.342	0.389	0.923	0.489	0.324	0.706
PyHCA	596	5	33	12	0.411	0.387	0.992	0.267	0.706	0.629
JRONN	595	6	33	12	0.397	0.381	0.99	0.267	0.667	0.628
MobiDB-lite	599	2	34	11	0.437	0.379	0.997	0.244	0.846	0.621
DisPredict-2	586	15	32	13	0.33	0.356	0.975	0.289	0.464	0.632
IUPred2A-short	599	2	35	10	0.413	0.351	0.997	0.222	0.833	0.609
S2D-2	572	29	30	15	0.288	0.337	0.952	0.333	0.341	0.643
PDB(observed)	468	133	13	32	0.286	0.305	0.779	0.711	0.194	0.745
AUCpreD-np	590	11	35	10	0.293	0.303	0.982	0.222	0.476	0.602
ESpritz-X	595	6	36	9	0.321	0.3	0.99	0.2	0.6	0.595
FoldUnfold	456	145	14	31	0.256	0.281	0.759	0.689	0.176	0.724
DISOPRED-3.1	596	5	39	6	0.246	0.214	0.992	0.133	0.545	0.563

DisEMBL-HL	601	0	41	4	0.288	0.163	1	0.089	1	0.544
PDB(remote)	590	11	42	3	0.085	0.102	0.982	0.067	0.214	0.524
DisEMBL-465	601	0	43	2	0.204	0.085	1	0.044	1	0.522
PDB(close)	589	12	43	2	0.043	0.068	0.98	0.044	0.143	0.512
Conservation	441	160	38	7	-0.064	0.066	0.734	0.156	0.042	0.445
DynaMine	601	0	45	0	0	0	1	0	0	0.5
GlobPlot	601	0	45	0	0	0	1	0	0	0.5
DFLpred	601	0	45	0	0	0	1	0	0	0.5

Supplemental Table 3. CAID scores taken from (Necci et al., 2021). This table is provided in a .xlsx format at the manuscript's GitHub repository.

Rankings

Rank	MCC	F1	BAC	PPV
1	flDPnn	flDPnn	Gene3D	DisEMBL-HL
2	RawMSA	RawMSA	flDPnn	DisEMBL-465
3	**metapredict**	**metapredict**	RawMSA	MobiDB-lite
4	Predisorder	VSL2B	flDPlr	IUPred2A-short
5	VSL2B	flDPlr	DisoMine	ESpritz-N
6	flDPlr	Predisorder	PDB(observed)	**metapredict**
7	SPOT-Disorder-Single	SPOT-Disorder1	VSL2B	PyHCA
8	MobiDB-lite	DisoMine	FoldUnfold	IUPred2A-long
9	AUCpreD	AUCpreD	SPOT-Disorder1	SPOT-Disorder-Single
10	ESpritz-N	SPOT-Disorder2	**metapredict**	JRONN
11	DisoMine	SPOT-Disorder-Single	SPOT-Disorder2	flDPnn
12	IUPred2A-long	IsUnstruct	ESpritz-D	Predisorder
13	SPOT-Disorder1	IUPred2A-long	Predisorder	ESpritz-X
14	IUPred2A-short	Gene3D	AUCpreD	RawMSA
15	IsUnstruct	ESpritz-N	IsUnstruct	AUCpreD
16	PyHCA	ESpritz-D	SPOT-Disorder-Single	IsUnstruct
17	SPOT-Disorder2	PyHCA	S2D-2	DISOPRED-3.1
18	JRONN	JRONN	IUPred2A-long	VSL2B
19	Gene3D	MobiDB-lite	DisPredict-2	AUCpreD-np
20	ESpritz-D	DisPredict-2	ESpritz-N	DisPredict-2
21	DisPredict-2	IUPred2A-short	PyHCA	SPOT-Disorder2
22	ESpritz-X	S2D-2	JRONN	flDPlr
23	AUCpreD-np	PDB(observed)	MobiDB-lite	SPOT-Disorder1
24	S2D-2	AUCpreD-np	IUPred2A-short	DisoMine
25	DisEMBL-HL	ESpritz-X	AUCpreD-np	S2D-2
26	PDB(observed)	FoldUnfold	ESpritz-X	ESpritz-D
27	FoldUnfold	DISOPRED-3.1	DISOPRED-3.1	Gene3D

28	DISOPRED-3.1	DisEMBL-HL	DisEMBL-HL	PDB(remote)
29	DisEMBL-465	PDB(remote)	PDB(remote)	PDB(observed)
30	PDB(remote)	DisEMBL-465	DisEMBL-465	FoldUnfold
31	PDB(close)	PDB(close)	PDB(close)	PDB(close)
32	DynaMine	Conservation	DynaMine	Conservation
33	GlobPlot	DynaMine	GlobPlot	DynaMine
34	DFLpred	GlobPlot	DFLpred	GlobPlot
35	Conservation	DFLpred	Conservation	DFLpred

Supplemental Table 4. CAID-based rankings. This table is provided in a .xlsx format at the manuscript's GitHub repository.

	BAC	F1-S	FPR	MCC	PPV	TPR	TNR
flDPnn	0.72	0.483	0.189	0.37	0.392	0.629	0.811
SPOT-Disorder2	0.725	0.469	0.343	0.349	0.333	0.794	0.657
flDPlr	0.693	0.452	0.184	0.33	0.374	0.57	0.816
RawMSA	0.714	0.445	0.297	0.328	0.321	0.725	0.703
Predisorder	0.691	0.435	0.28	0.301	0.324	0.661	0.72
SPOT-Disorder1	0.723	0.434	0.386	0.33	0.294	0.832	0.614
AUCpreD	0.712	0.433	0.376	0.318	0.297	0.801	0.624
SPOT-Disorder-Single	0.71	0.432	0.341	0.315	0.302	0.76	0.659
ESpritz-D	0.703	0.428	0.325	0.307	0.303	0.731	0.675
AUCpreD-np	0.699	0.424	0.327	0.301	0.3	0.725	0.673
DisoMine	0.698	0.424	0.326	0.299	0.3	0.721	0.674
metapredict	0.693	0.421	0.320	0.293	0.300	0.705	0.680
IUPred2A-short	0.688	0.42	0.297	0.29	0.305	0.674	0.703
MobiDB-lite	0.688	0.42	0.296	0.289	0.305	0.673	0.704
IUPred-long	0.686	0.418	0.294	0.287	0.305	0.666	0.706
IUPred-short	0.688	0.418	0.304	0.288	0.302	0.679	0.696
ESpritz-X	0.689	0.418	0.309	0.288	0.301	0.686	0.691
IsUnstruct	0.689	0.418	0.311	0.288	0.3	0.688	0.689
IUPred2A-long	0.685	0.416	0.299	0.285	0.302	0.67	0.701
VSL2B	0.684	0.408	0.341	0.277	0.286	0.709	0.659
JRONN	0.672	0.401	0.318	0.263	0.287	0.663	0.682
ESpritz-N	0.664	0.4	0.271	0.259	0.3	0.599	0.729
DISOPRED-3.1	0.674	0.393	0.401	0.258	0.266	0.749	0.599
PyHCA	0.66	0.385	0.346	0.241	0.271	0.666	0.654
DynaMine	0.66	0.384	0.362	0.24	0.267	0.682	0.638
Gene3D	0.653	0.368	0.486	0.226	0.24	0.791	0.514
FoldUnfold	0.642	0.365	0.382	0.211	0.251	0.666	0.618
DisEMBL-465	0.627	0.363	0.215	0.214	0.296	0.468	0.785

S2D-1	0.633	0.361	0.329	0.203	0.259	0.595	0.671
PDB (close)	0.637	0.353	0.38	0.202	0.242	0.655	0.62
S2D-2	0.624	0.347	0.439	0.183	0.232	0.687	0.561
PDB (observed)	0.616	0.339	0.565	0.174	0.215	0.796	0.435
DisPredict-2	0.599	0.326	0.326	0.152	0.237	0.523	0.674
PDB (remote)	0.614	0.321	0.45	0.163	0.21	0.678	0.55
GlobPlot	0.587	0.312	0.253	0.143	0.246	0.427	0.747
Conservation	0.552	0.288	0.483	0.077	0.191	0.587	0.517
DisEMBL-HL	0.577	0.286	0.099	0.172	0.33	0.253	0.901
DFLpred	0.503	0.025	0.008	0.022	0.249	0.013	0.992

Supplemental Table 5. CAID per-residue assessment using DisProt dataset. This table is provided in a .xlsx format at the manuscript's GitHub repository.

Rankings

Rank	MCC	F1	BAC	PPV
1	flDPnn	flDPnn	SPOT-Disorder2	flDPnn
2	SPOT-Disorder2	SPOT-Disorder2	SPOT-Disorder1	flDPlr
3	SPOT-Disorder1	flDPlr	flDPnn	SPOT-Disorder2
4	flDPlr	RawMSA	RawMSA	DisEMBL-HL
5	RawMSA	Predisorder	AUCpreD	Predisorder
6	AUCpreD	SPOT-Disorder1	SPOT-Disorder-Single	RawMSA
7	SPOT-Disorder-Single	AUCpreD	ESpritz-D	IUPred2A-short
8	ESpritz-D	SPOT-Disorder-Single	AUCpreD-np	MobiDB-lite
9	AUCpreD-np	ESpritz-D	DisoMine	IUPred-long
10	Predisorder	AUCpreD-np	flDPlr	ESpritz-D
11	DisoMine	DisoMine	**metapredict**	SPOT-Disorder-Single
12	**metapredict**	**metapredict**	Predisorder	IUPred-short
13	IUPred2A-short	IUPred2A-short	ESpritz-X	IUPred2A-long
14	MobiDB-lite	MobiDB-lite	IsUnstruct	ESpritz-X
15	ESpritz-X	ESpritz-X	IUPred2A-short	AUCpreD-np
16	IsUnstruct	IsUnstruct	MobiDB-lite	DisoMine
17	IUPred-short	IUPred-short	IUPred-short	IsUnstruct
18	IUPred-long	IUPred-long	IUPred-long	ESpritz-N
19	IUPred2A-long	IUPred2A-long	IUPred2A-long	**metapredict**
20	VSL2B	VSL2B	VSL2B	AUCpreD
21	JRONN	JRONN	DISOPRED-3.1	DisEMBL-465
22	ESpritz-N	ESpritz-N	JRONN	SPOT-Disorder1
23	DISOPRED-3.1	DISOPRED-3.1	ESpritz-N	JRONN
24	PyHCA	PyHCA	PyHCA	VSL2B
25	DynaMine	DynaMine	DynaMine	PyHCA
26	Gene3D	Gene3D	Gene3D	DynaMine

27	DisEMBL-465	FoldUnfold	FoldUnfold	DISOPRED-3.1
28	FoldUnfold	DisEMBL-465	PDB (close)	S2D-1
29	S2D-1	S2D-1	S2D-1	FoldUnfold
30	PDB (close)	PDB (close)	DisEMBL-465	DFLpred
31	S2D-2	S2D-2	S2D-2	GlobPlot
32	PDB (observed)	PDB (observed)	PDB (observed)	PDB (close)
33	DisEMBL-HL	DisPredict-2	PDB (remote)	Gene3D
34	PDB (remote)	PDB (remote)	DisPredict-2	DisPredict-2
35	DisPredict-2	GlobPlot	GlobPlot	S2D-2
36	GlobPlot	Conservation	DisEMBL-HL	PDB (observed)
37	Conservation	DisEMBL-HL	Conservation	PDB (remote)
38	DFLpred	DFLpred	DFLpred	Conservation

Supplemental Table 6. CAID per-residue rankings using DisProt dataset. This table is provided in a .xlsx format at the manuscript's GitHub repository.

	BAC	F1-S	FPR	MCC	PPV	TPR	TNR
PDB(observed)	0.898	0.886	0	0.854	1	0.796	1
SPOT-Disorder1	0.846	0.788	0.09	0.696	0.795	0.782	0.91
SPOT-Disorder2	0.836	0.784	0.055	0.706	0.851	0.727	0.945
AUCpreD	0.816	0.756	0.07	0.662	0.82	0.701	0.93
PDB (close)	0.811	0.755	0.033	0.689	0.891	0.655	0.967
SPOT-Disorder-Single	0.817	0.751	0.095	0.646	0.775	0.729	0.905
RawMSA	0.815	0.745	0.106	0.635	0.755	0.736	0.894
AUCpreD-np	0.797	0.725	0.092	0.615	0.769	0.686	0.908
DISOPRED-3.1	0.796	0.724	0.092	0.613	0.768	0.684	0.908
Predisorder	0.788	0.717	0.067	0.619	0.813	0.642	0.933
IUPred-long	0.783	0.704	0.096	0.588	0.754	0.661	0.904
fIDPnn	0.782	0.701	0.113	0.576	0.727	0.676	0.887
IsUnstruct	0.779	0.7	0.091	0.585	0.76	0.648	0.909
IUPred2A-long	0.776	0.697	0.087	0.584	0.766	0.64	0.913
VSL2B	0.774	0.695	0.087	0.581	0.765	0.636	0.913
ESpritz-X	0.778	0.695	0.119	0.566	0.717	0.675	0.881
IUPred-short	0.775	0.693	0.104	0.571	0.738	0.654	0.896
DisoMine	0.78	0.693	0.16	0.55	0.668	0.721	0.84
Gene3D	0.785	0.692	0.22	0.539	0.615	0.791	0.78
IUPred2A-short	0.773	0.691	0.094	0.574	0.752	0.64	0.906
ESpritz-D	0.778	0.69	0.166	0.544	0.66	0.723	0.834
metapredict	0.791	0.712	0.124	0.585	0.718	0.705	0.876
MobiDB-lite	0.764	0.683	0.063	0.583	0.806	0.592	0.937
fIDPlr	0.761	0.671	0.119	0.537	0.705	0.641	0.881
ESpritz-N	0.751	0.662	0.073	0.554	0.779	0.575	0.927
JRONN	0.751	0.661	0.081	0.546	0.762	0.583	0.919
DynaMine	0.739	0.641	0.11	0.505	0.704	0.588	0.89
FoldUnfold	0.736	0.636	0.193	0.462	0.608	0.666	0.807

PyHCA	0.731	0.629	0.107	0.494	0.704	0.569	0.893
S2D-1	0.724	0.617	0.089	0.494	0.728	0.536	0.911
S2D-2	0.703	0.591	0.253	0.386	0.536	0.658	0.747
PDB (remote)	0.703	0.579	0.273	0.377	0.505	0.678	0.727
DisEMBL-465	0.694	0.57	0.11	0.426	0.667	0.498	0.89
DisEMBL-HL	0.641	0.535	0.47	0.262	0.415	0.752	0.53
DisPredict-2	0.625	0.491	0.285	0.24	0.455	0.534	0.715
Conservation	0.618	0.485	0.296	0.227	0.445	0.533	0.704
GlobPlot	0.641	0.48	0.111	0.328	0.613	0.394	0.889
DFLpred	0.504	0.027	0.005	0.043	0.53	0.014	0.995

Supplemental Table 7. CAID per-residue rankings using DisProt-PDB dataset. This table is provided in a .xlsx format at the manuscript's GitHub repository.

Rankings

Rank	MCC	F1	BAC	PPV
1	PDB(observed)	PDB(observed)	PDB(observed)	PDB(observed)
2	SPOT-Disorder2	SPOT-Disorder1	SPOT-Disorder1	PDB (close)
3	SPOT-Disorder1	SPOT-Disorder2	SPOT-Disorder2	SPOT-Disorder2
4	PDB (close)	AUCpreD	SPOT-Disorder-Single	AUCpreD
5	AUCpreD	PDB (close)	AUCpreD	Predisorder
6	SPOT-Disorder-Single	SPOT-Disorder-Single	RawMSA	MobiDB-lite
7	RawMSA	RawMSA	PDB (close)	SPOT-Disorder1
8	Predisorder	AUCpreD-np	AUCpreD-np	ESpritz-N
9	AUCpreD-np	DISOPRED-3.1	DISOPRED-3.1	SPOT-Disorder-Single
10	DISOPRED-3.1	Predisorder	**metapredict**	AUCpreD-np
11	IUPred-long	**metapredict**	Predisorder	DISOPRED-3.1
12	IsUnstruct	IUPred-long	Gene3D	IUPred2A-long
13	**metapredict**	flDPnn	IUPred-long	VSL2B
14	IUPred2A-long	IsUnstruct	flDPnn	JRONN
15	MobiDB-lite	IUPred2A-long	DisoMine	IsUnstruct
16	VSL2B	VSL2B	IsUnstruct	RawMSA
17	flDPnn	ESpritz-X	ESpritz-X	IUPred-long
18	IUPred2A-short	IUPred-short	ESpritz-D	IUPred2A-short
19	IUPred-short	DisoMine	IUPred2A-long	IUPred-short
20	ESpritz-X	Gene3D	IUPred-short	S2D-1
21	ESpritz-N	IUPred2A-short	VSL2B	flDPnn
22	DisoMine	ESpritz-D	IUPred2A-short	**metapredict**
23	JRONN	MobiDB-lite	MobiDB-lite	ESpritz-X
24	ESpritz-D	flDPlr	flDPlr	flDPlr
25	Gene3D	ESpritz-N	ESpritz-N	DynaMine
26	flDPlr	JRONN	JRONN	PyHCA
27	DynaMine	DynaMine	DynaMine	DisoMine

28	PyHCA	FoldUnfold	FoldUnfold	DisEMBL-465
29	S2D-1	PyHCA	PyHCA	ESpritz-D
30	FoldUnfold	S2D-1	S2D-1	Gene3D
31	DisEMBL-465	S2D-2	S2D-2	GlobPlot
32	S2D-2	PDB (remote)	PDB (remote)	FoldUnfold
33	PDB (remote)	DisEMBL-465	DisEMBL-465	S2D-2
34	GlobPlot	DisEMBL-HL	DisEMBL-HL	DFLpred
35	DisEMBL-HL	DisPredict-2	GlobPlot	PDB (remote)
36	DisPredict-2	Conservation	DisPredict-2	DisPredict-2
37	Conservation	GlobPlot	Conservation	Conservation
38	DFLpred	DFLpred	DFLpred	DisEMBL-HL

Supplemental Table 8. CAID per-residue rankings using DisProt-PDB dataset. This table is provided in a .xlsx format at the manuscript's GitHub repository.

Supplemental Figures

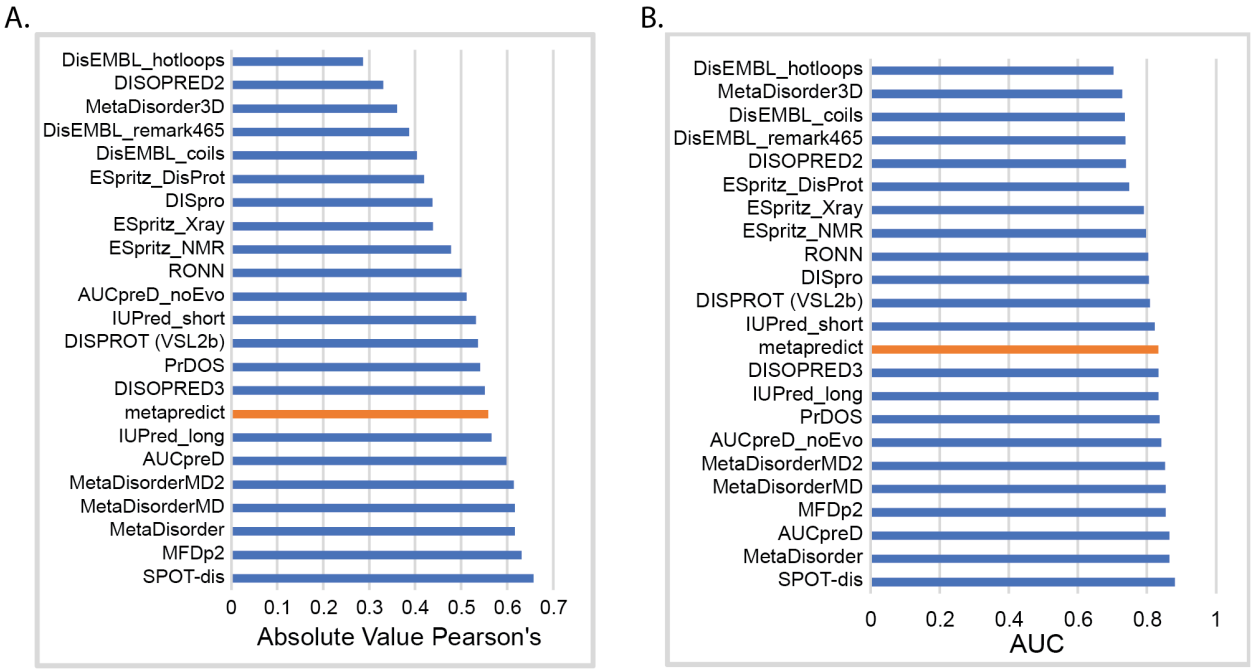

Supplemental Figure 1. Evaluation of metapredict using CheZOD scores. (A) The absolute value of the Pearson's correlation coefficient calculated by comparing the correlation between each predictor's score per residue and the CheZOD score. **(B)** The area under the receiver operating characteristic curve (AUC) (generated by comparing disorder scores of various predictors to disorder predictions from CheZOD scores. Values for all predictors in (A) and (B) other than metapredict (orange bar) were obtained from (Nielsen & Mulder, 2019).

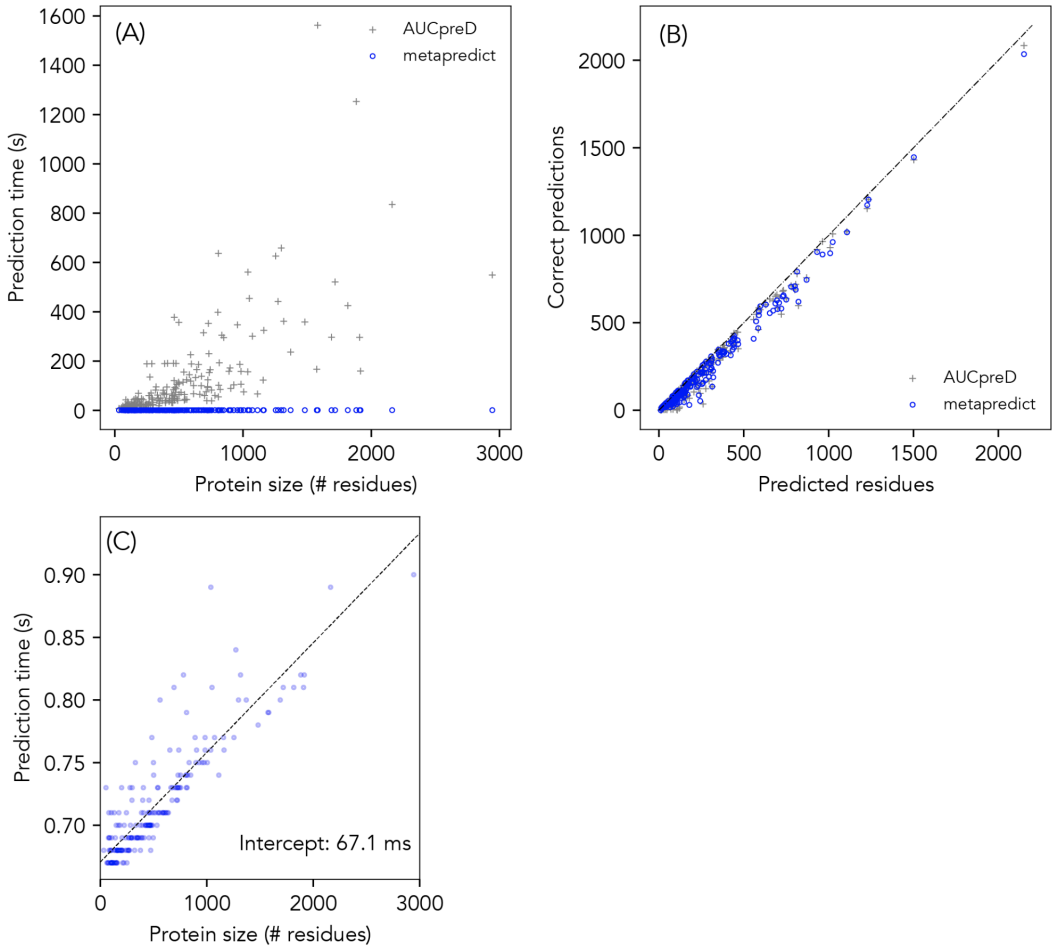

Supplemental Figure 2. Comparison of execution time and predict performance for AUCPreD vs. metapredict (A) Run time of 200 different proteins from the DISPROT dataset spanning a variety of different sizes as assessed by AUCPreD (grey crosses) vs. metapredict (blue circles). Both methods show a clear correlation between sequence length and execution time (AUCPreD Pearson's correlation coefficient of 0.71, metapredict Pearson's correlation coefficient of 0.88), yet the magnitude of the execution time for metapredict makes it look effectively flat. **(B)** Comparison of accuracy between AUCPreD and metapredict for the same sequences. The two methods are effectively comparable (see also **Fig. 3A**). **(C)** Zoomed-in comparison of execution time vs. protein size for metapredict. Note that the intercept here is 670 ms, which reflects the time needed to read-in and load the trained network, while the actual per-sequence execution time is under 100 ms for even a 1000 residue sequence (see also **Supplemental Fig. 8** where execution times are calculated after the initial network file has been read in and parsed by metapredict).

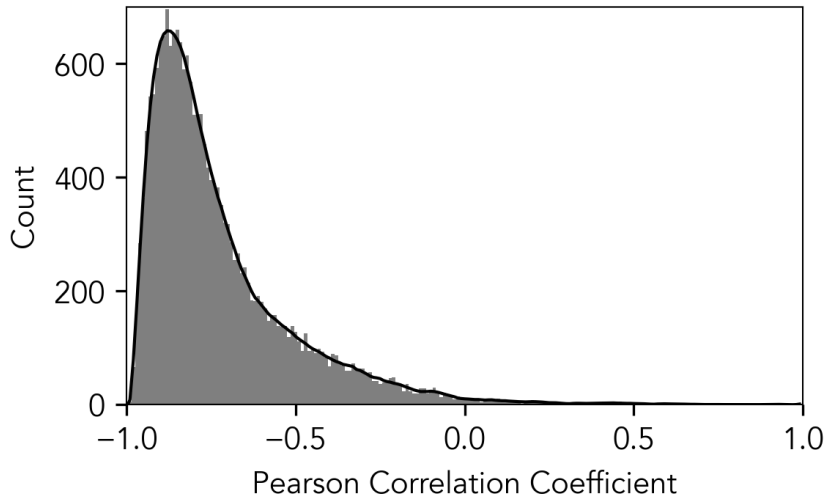

Supplemental Figure 3. Disorder and predicted structure confidence are highly correlated but independent measures of (lack of) protein structure.

We analyzed every sequence in the human proteome, computed per-residue disorder predictions and predicted structure confidence scores (predicted pLDDT), and correlated the scores using the Pearson correlation coefficient. The histogram above represents the overall distribution of those correlation coefficients calculated for 20,394 protein sequences.

A.

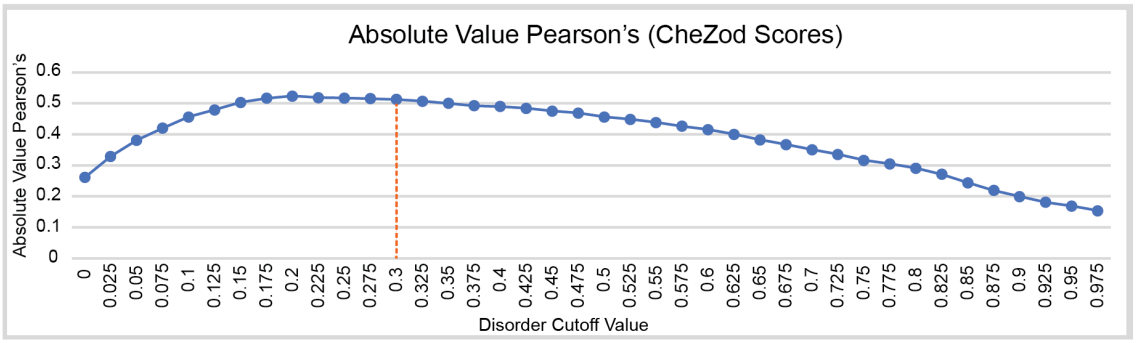

B.

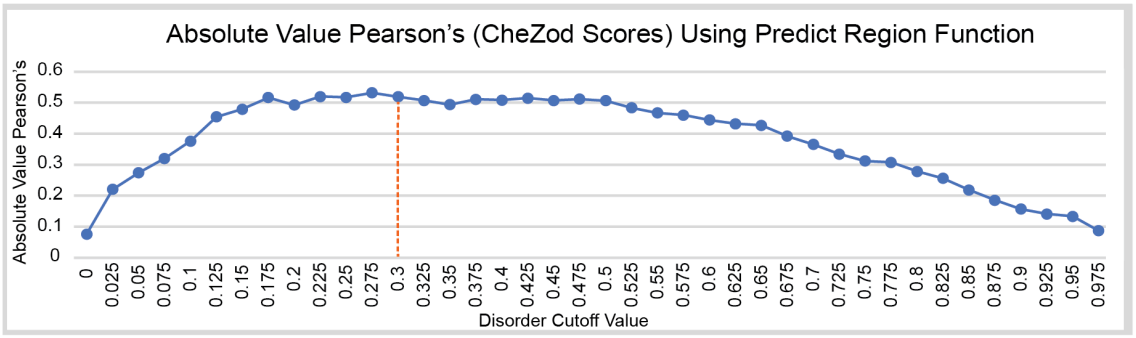

Supplemental Figure 4. Assessing the impact of disorder cutoff values on binary order and disorder classification of CheZOD data. (A) Absolute value of Pearson's Correlation Coefficient for binary predictions of disorder by metapredict compared to binary classifications of disorder from the CheZOD dataset. **(B)** Absolute value of Pearson's Correlation Coefficient for binary predictions of disorder by metapredict where the binary predictions were obtained using the predict_disorder_domains() function. These predictions are compared to binary classifications of disorder from CheZOD dataset. For both (A) and (B), the orange line represents the cutoff value used for binary classifications of order and disorder for metapredict.

A.

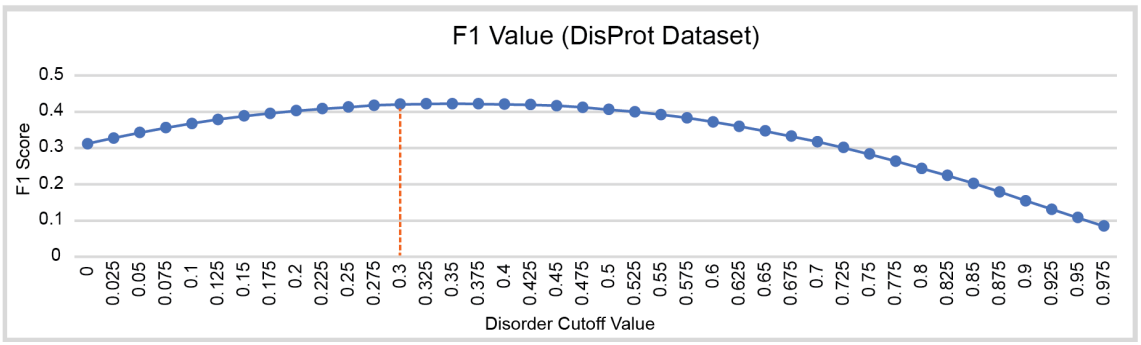

B.

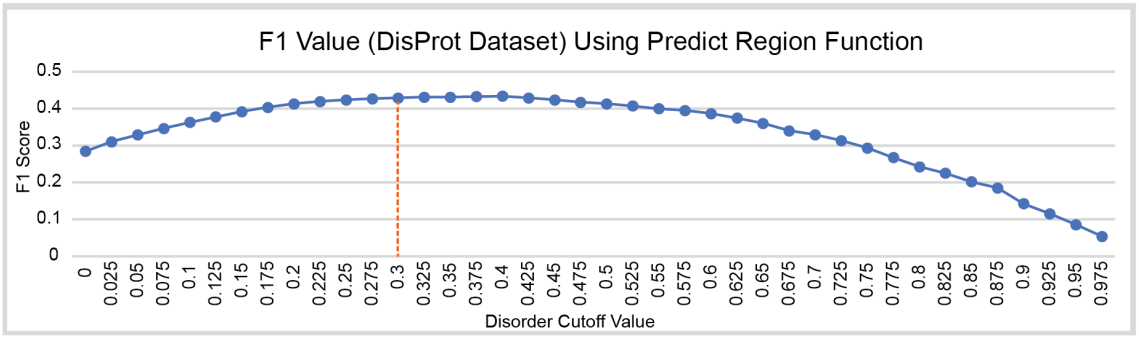

Supplemental Figure 5. Assessing the impact of disorder cutoff values on binary order and disorder classification of the Disprot Dataset (CAID). (A) F1-scores for binary predictions of disorder by metapredict compared to binary classifications of disorder from the Disprot dataset. **(B)** F1-scores for binary predictions of disorder by metapredict where the binary predictions were obtained using the predict_disorder_domains() function. These predictions were compared to binary classifications of disorder from the Disprot dataset. For both (A) and (B), the orange line represents the cutoff value used for binary classifications of order and disorder for metapredict.

A.

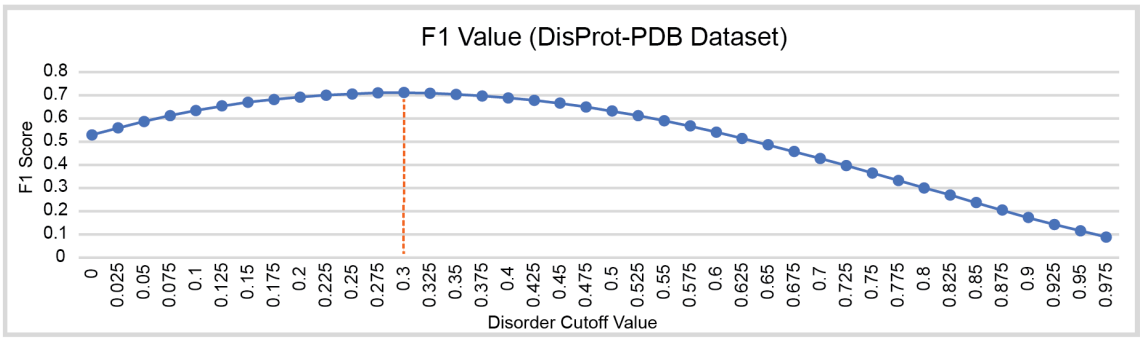

B.

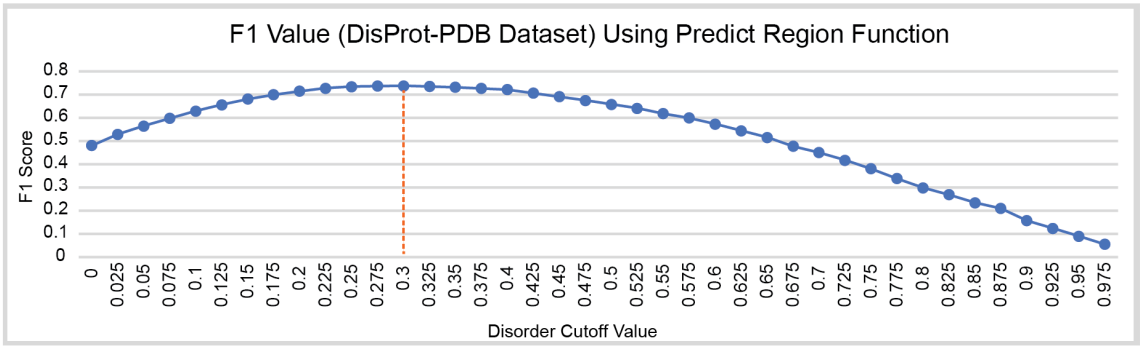

Supplemental Figure 6. Assessing the impact of disorder cutoff values on binary order and disorder classification of the Disprot Dataset-PDB (CAID). (A) F1-scores for binary predictions of disorder by metapredict compared to binary classifications of disorder from the Disprot-PDB dataset. **(B)** F1-scores for binary predictions of disorder by metapredict where the binary predictions were obtained using the predict_disorder_domains() function. These predictions were compared to binary classifications of disorder from the Disprot-PDB dataset. For both (A) and (B), the orange line represents the cutoff value used for binary classifications of order and disorder for metapredict.

A.

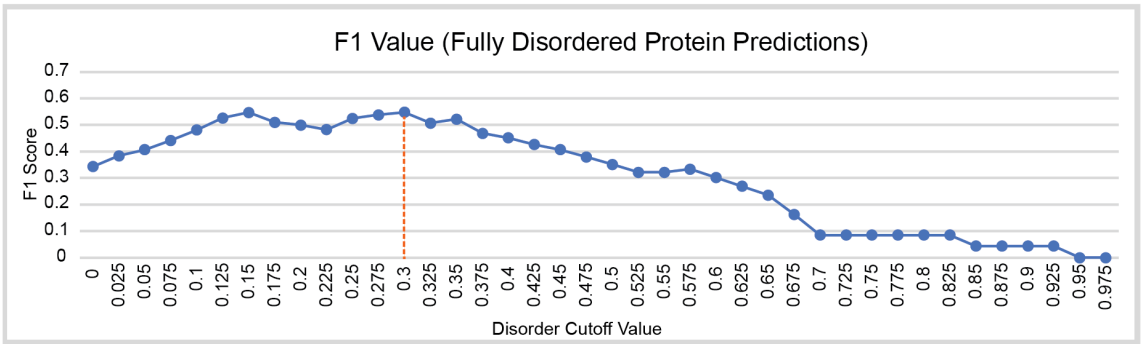

B.

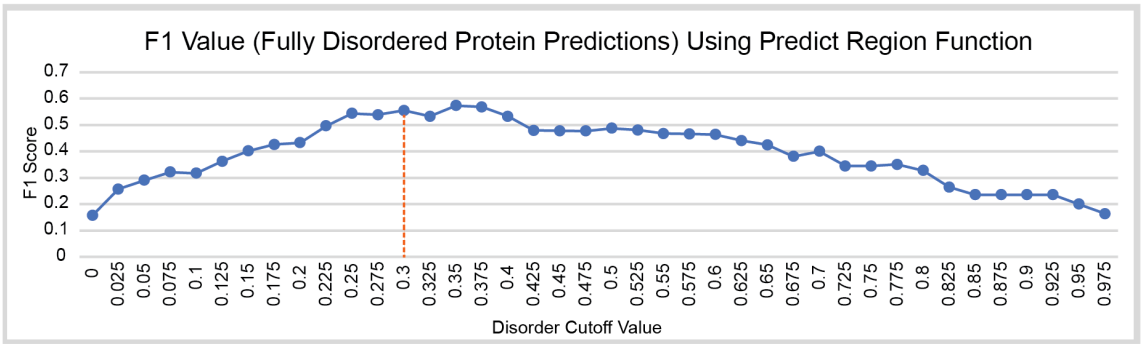

Supplemental Figure 7. Assessing the impact of disorder cutoff values on metapredict identifying fully disordered proteins from the Disprot Dataset (CAID). (A) F1-scores for predicted fully disordered proteins by metapredict compared to the known number of fully disordered proteins in the Disprot dataset. **(B)** F1-scores for predicted fully disordered proteins by metapredict where the binary predictions used to classify a protein as fully disordered were obtained using the predict_disorder_domains() function. These predictions were compared to the known number of fully disordered proteins in the Disprot dataset. For both (A) and (B), fully disordered proteins were counted if the predictor classified at least 95% of residues within a protein as disordered. For both (A) and (B), the orange line represents the cutoff value used for binary classifications of order and disorder for metapredict.

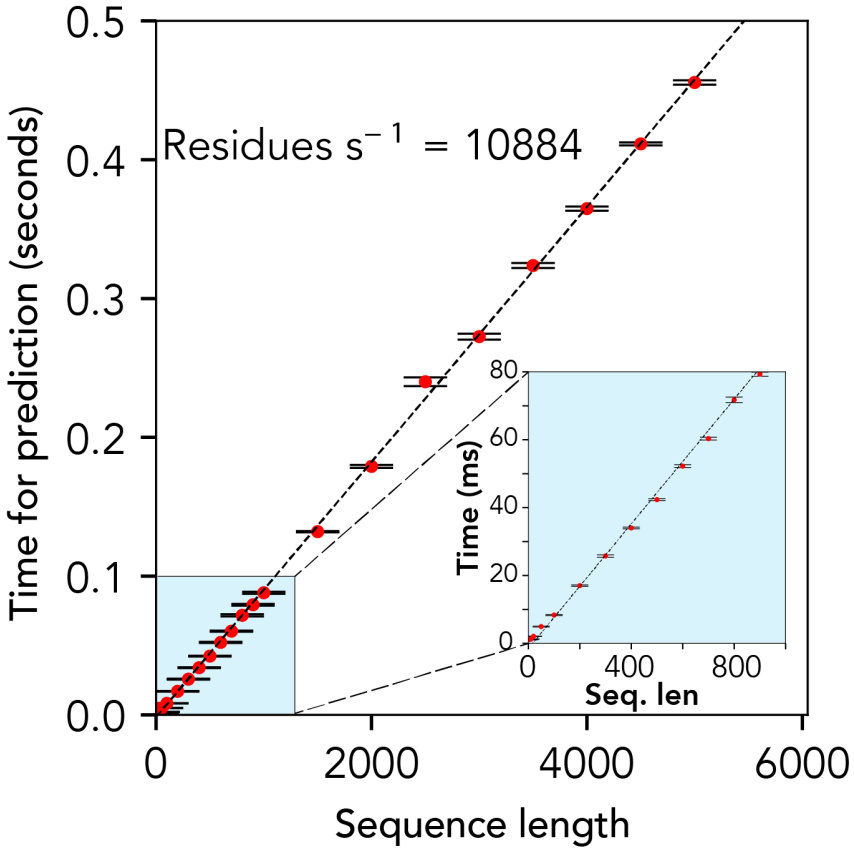

Supplemental Figure 8. Metapredict performance as a function of sequence length in number of residues. Assessment of length-dependence of metapredict performance reveals a linear scaling of prediction time with sequence length. Sequences here are randomly generated fixed-length sequences. Error bars are standard error of the mean calculated over thirty independent runs for random sequences of the specified length. Code for this analysis is provided in the Supporting Data GitHub repository.

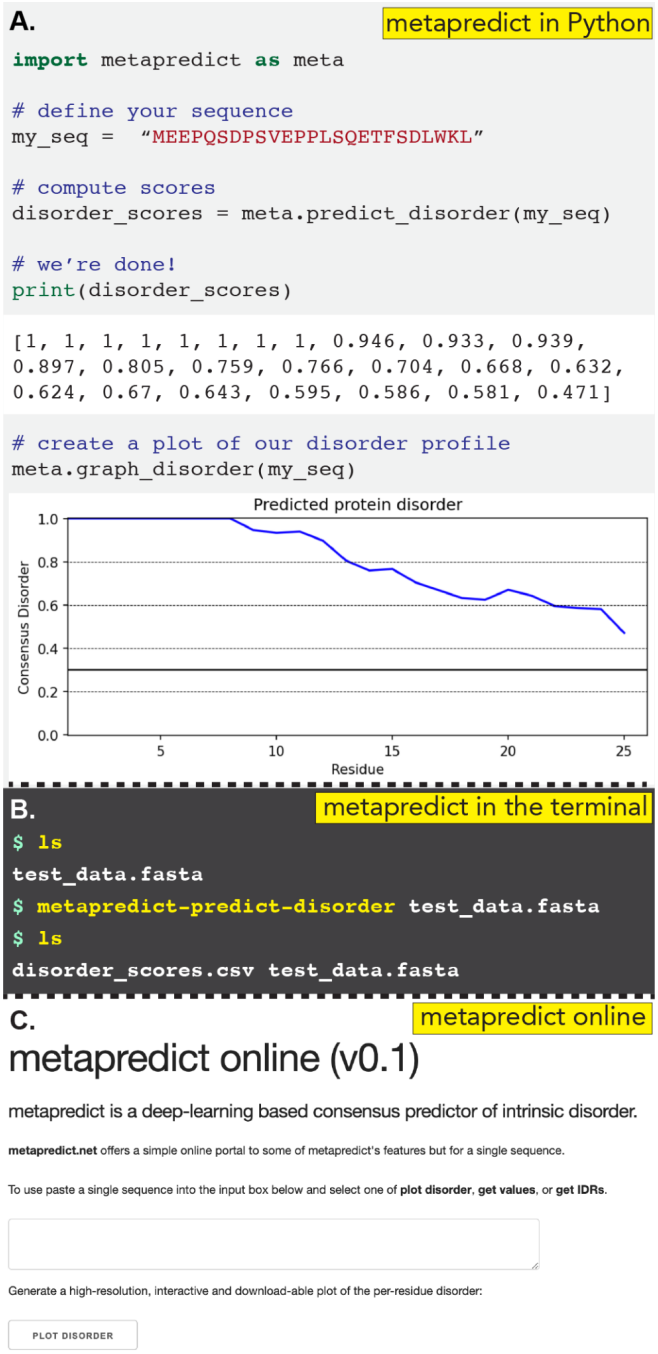

Supplemental Figure 9. Metapredict offers three distinct modes of use. (A) Metapredict can be used as a Python library, with simple and intuitive integration into existing Python code or for exploration in a Jupyter notebook. **(B)** Metapredict can be used as a command-line tool to interact directly with FASTA files. The file generated by the command metapredict-predict-disorder ("disorder_scores.csv") is a simple comma separated value (CSV) file with per-residue disorder values provided for each sequence in the FASTA file. **(C)** Finally, metapredict is offered as a simple web server (https://metapredict.net), which can generate high-quality downloadable figures or allow per-residue disorder scores to be obtained as a CSV data file.

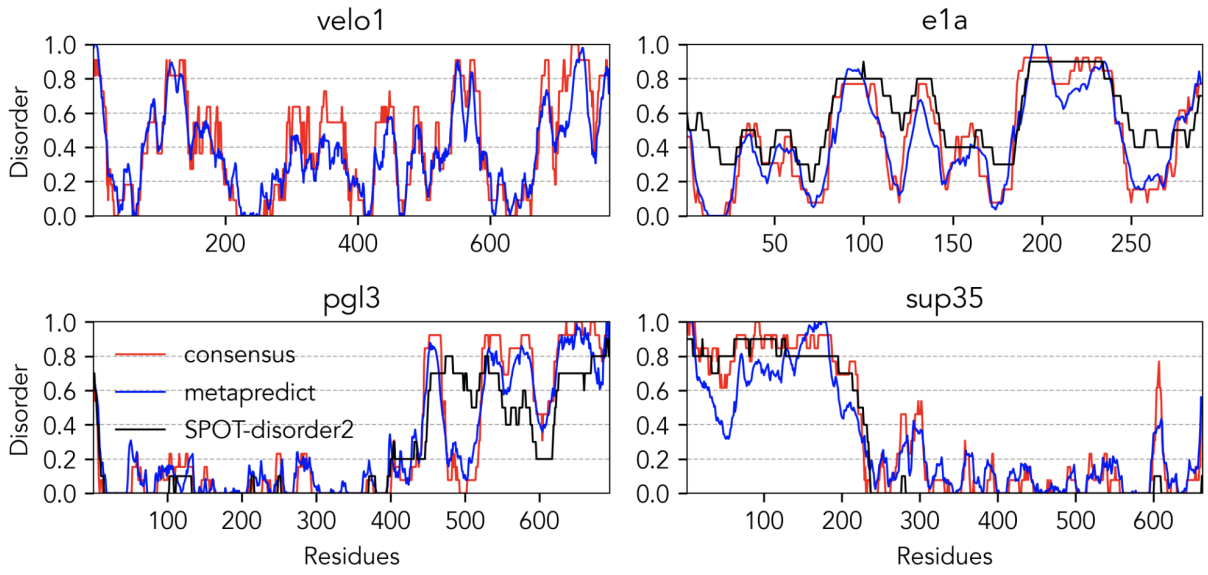

Supplemental Figure 10. Metapredict accurately recapitulates precomputed consensus disorder scores. Precomputed consensus disorder scores from the MobiDB database (red) and predicted disorder scores obtained SPOT-disorder2 (black) are compared to predicted consensus disorder scores calculated by metapredict for Velo1 from *Xenopus laevis* (UniProt Q7T226), PGL-3 from *Caenorhabditis elegans* (UniProt G5EBV6), Early E1A protein from Human adenovirus C serotype 5 (UniProt P03255), and Sup35 from *Schizosaccharomyces pombe* (UniProt O74718). None of these proteins were part of the training, test, or validation set for metapredicts. Note that Velo1 exceeds the length that SPOT-disorder2 can be used on.

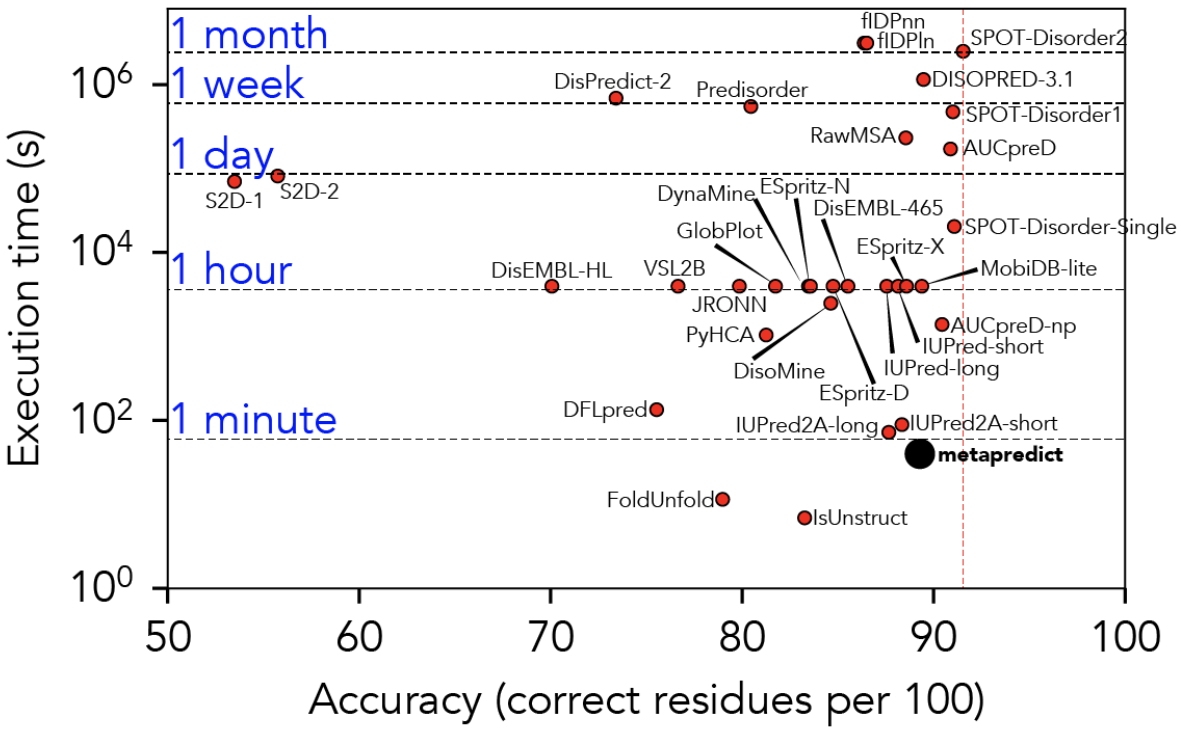

Supplemental Figure 11. Reproduction of **Fig. 3B** with various predictors explicitly labelled.

Supplemental References

Acids Research, N., & 2021. (2021). UniProt: The universal protein knowledgebase in 2021. *Nucleic Acids Research*, *49*(D1), D480–D489.

Griffith, D., & Holehouse, A. S. (2021). PARROT: a flexible recurrent neural network framework for analysis of large protein datasets. In *bioRxiv* (p. 2021.05.21.445045). https://doi.org/10.1101/2021.05.21.445045

Necci, M., Piovesan, D., CAID Predictors, DisProt Curators, & Tosatto, S. C. E. (2021). Critical assessment of protein intrinsic disorder prediction. *Nature Methods*. https://doi.org/10.1038/s41592-021-01117-3

Nielsen, J. T., & Mulder, F. A. A. (2019). Quality and bias of protein disorder predictors. *Scientific Reports*, *9*(1), 1–11.

Paszke, A., Gross, S., Massa, F., Lerer, A., Bradbury, J., Chanan, G., Killeen, T., Lin, Z., Gimelshein, N., Antiga, L., Desmaison, A., Köpf, A., Yang, E., DeVito, Z., Raison, M., Tejani, A., Chilamkurthy, S., Steiner, B., Fang, L., … Chintala, S. (2019). PyTorch: An Imperative Style, High-Performance Deep Learning Library. In *arXiv [cs.LG]*. arXiv. http://arxiv.org/abs/1912.01703

Piovesan, D., Necci, M., Escobedo, N., Monzon, A. M., Hatos, A., Mičetić, I., Quaglia, F., Paladin, L., Ramasamy, P., Dosztányi, Z., Vranken, W. F., Davey, N. E., Parisi, G., Fuxreiter, M., & Tosatto, S. C. E. (2021). MobiDB: intrinsically disordered proteins in 2021. *Nucleic Acids Research*, *49*(D1), D361–D367.

UniProt Consortium. (2019). UniProt: a worldwide hub of protein knowledge. *Nucleic Acids Research*, *47*(D1), D506–D515.